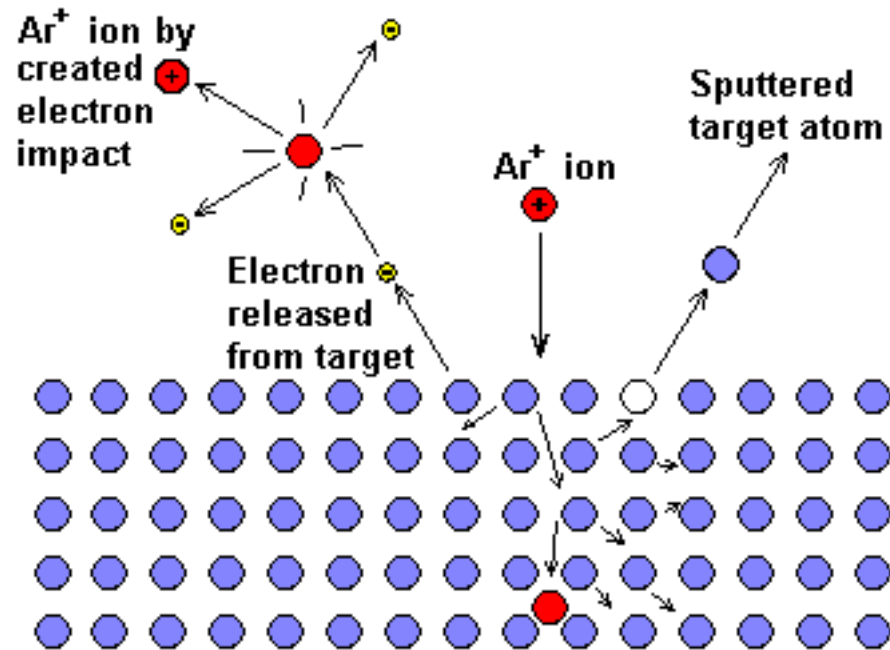


Francesco Ruffino (francesco.ruffino@ct.infn.it)

*Dipartimento di Fisica e Astronomia, Università di Catania, via S. Sofia 64, 95123
Catania, Italy*

CNR-IMM MATIS via S. Sofia 64, 95123 Catania, Italy

Sputtering Thin Films Deposition



Literature:

*1.A) K. Wasa, M. Kitabatake, H. Adachi, Thin Film Materials Technology, Cap. 1, Cap. 2, **Cap. 3**, **Cap. 4**, Cap. 7*

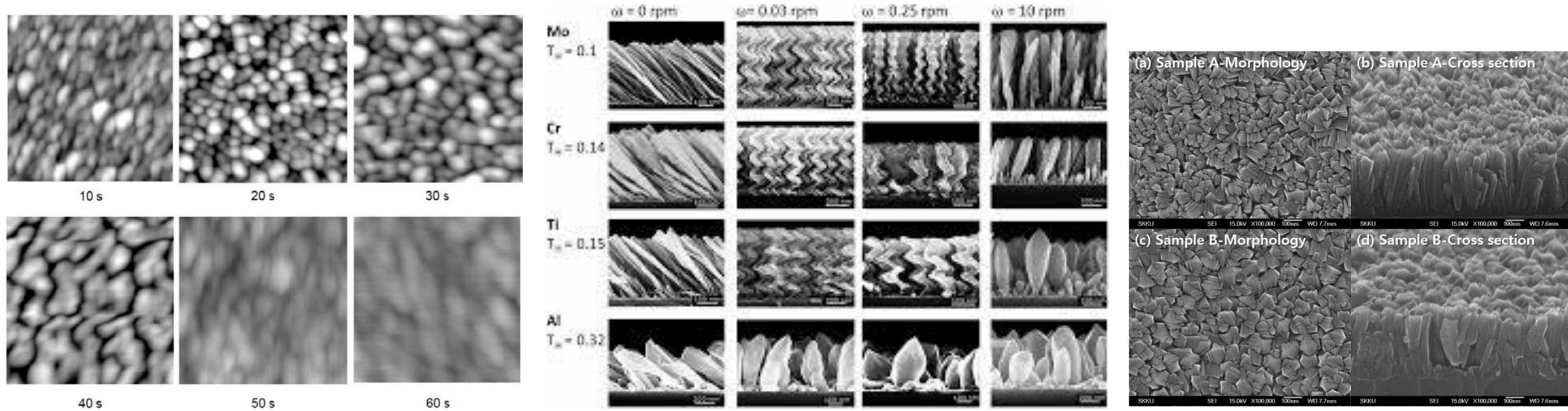
*1.B) P. M. Martin, Handbook of Deposition Technologies for Films and Coatings, Cap. 1, Cap. 2, Cap. 4, **Cap. 5**, Cap. 12, Cap. 15, Cap. 16*

Additional

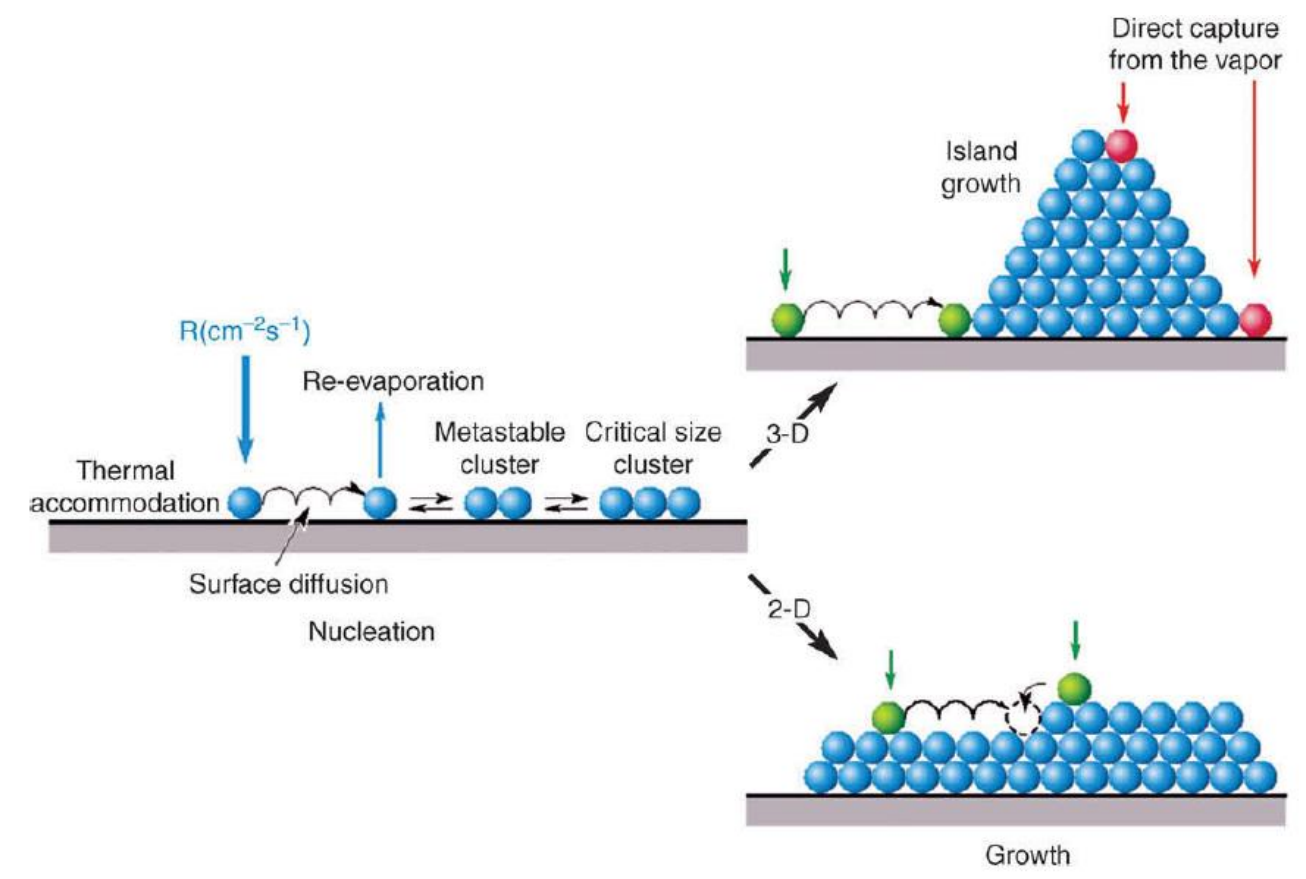
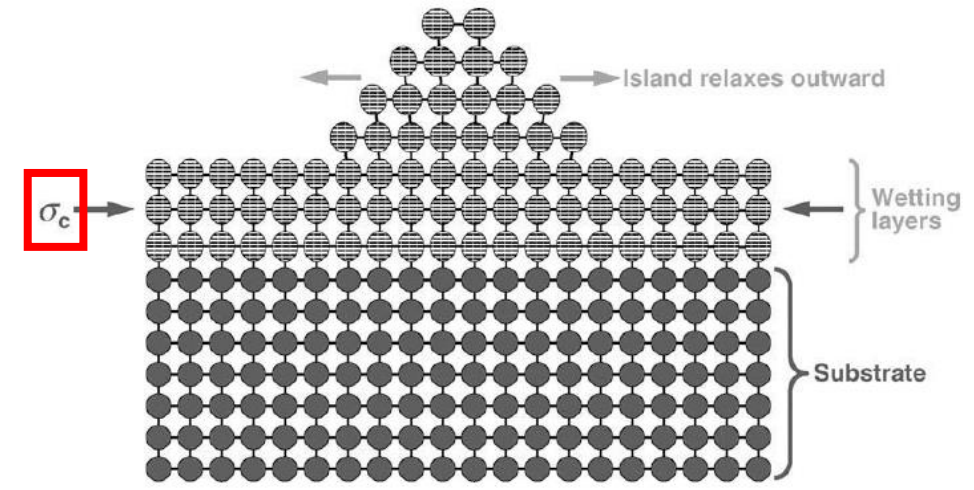
2) K. S. S. Harsha, Principles of Physical Vapor Deposition of Thin Films

Thin Films and Nanostructures

Engineered materials are the future of thin film technology. Engineered structures such as superlattices, nanolaminates, nanotubes, nanocomposites, smart materials, photonic bandgap materials, molecularly doped polymers, and structured materials all have the capacity to expand and increase the functionality of thin films and coatings used in a variety of applications and provide new applications. New advanced deposition processes and hybrid processes are being used and developed to deposit advanced thin film materials and structures not possible with conventional techniques a decade ago.



Coverage Mechanism	$\theta < 1$ ML	$1 < \theta < 2$ ML	$\theta > 2$ ML	Examples
3D island growth				Metals on SiO_2
2D layer growth				Cu/Cu, Si/Si, GaAs/GaAs
S-K growth				In/Si, Ge/Si, InGaAs/GaAs



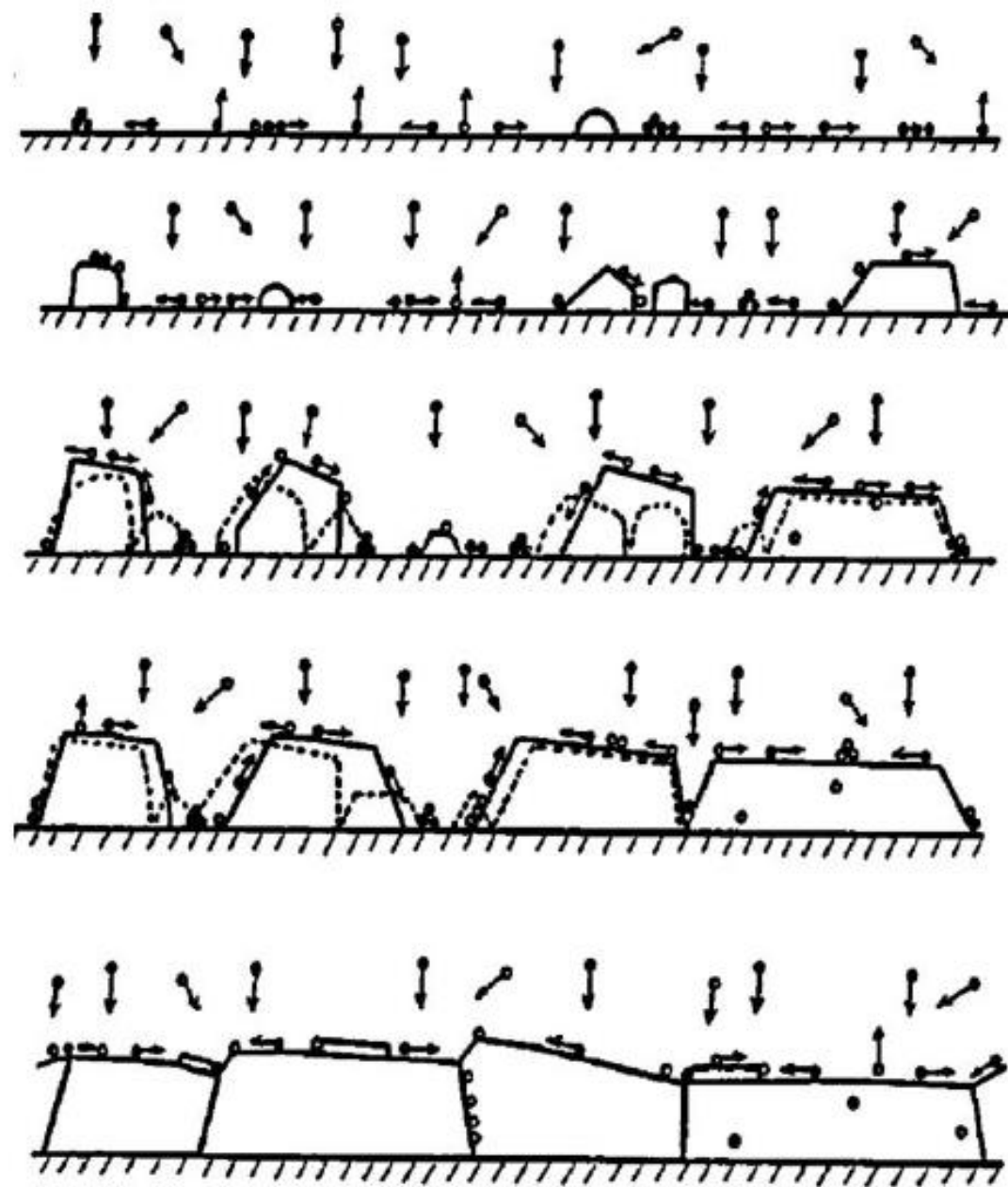


Figure 4.46: Schematic diagram illustrating fundamental growth processes controlling microstructural evolution [171, 172].

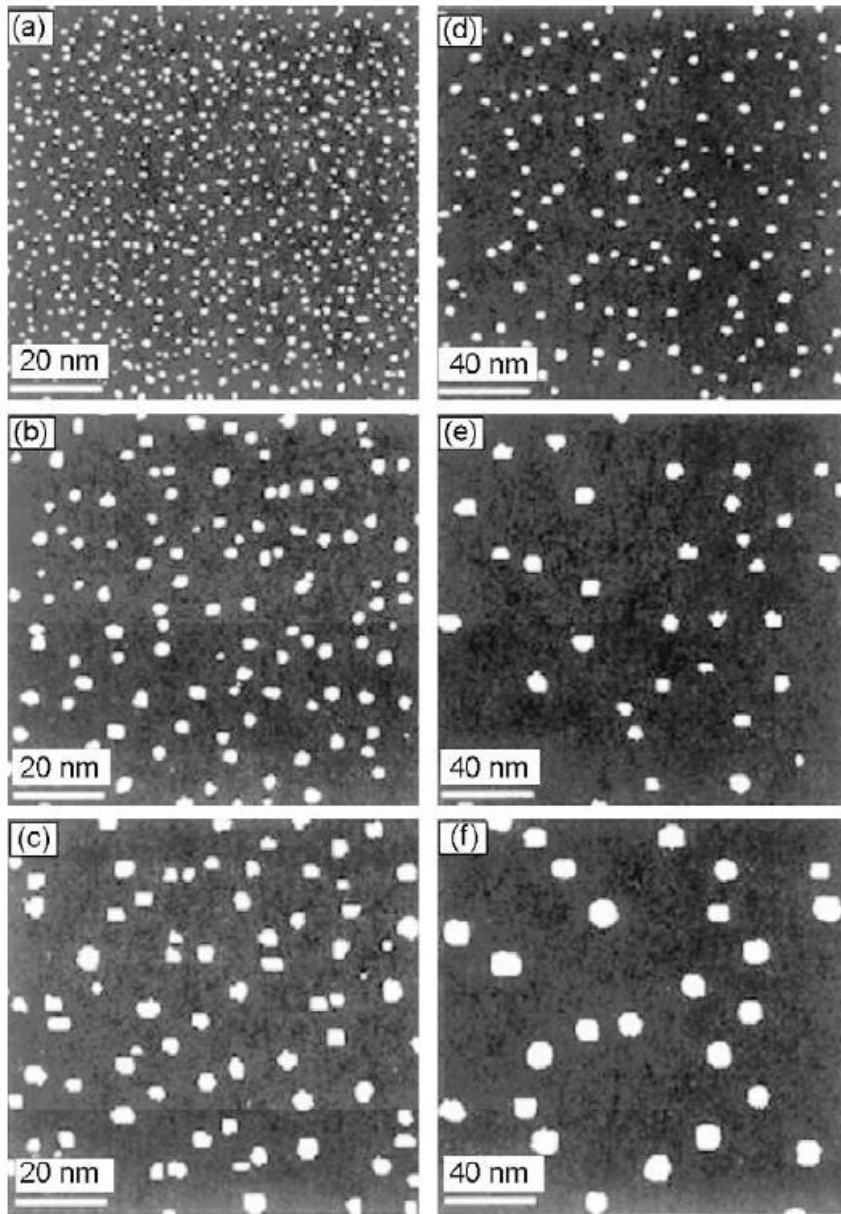


Figure 12.5: In situ STM images of Fe islands deposited on Fe(001) by MBE with a **flux** $J_{\text{Au}} = 1 \times 10^{13} \text{ cm}^{-2} \text{ s}^{-1}$ to a coverage $\theta_{\text{Fe}} = 0.07 \text{ ML}$ at temperatures $T_s =$ (a) 20, (b) 108, (c) 163, (d) 256, (e) 301, and (f) 356 °C. (From [29].)

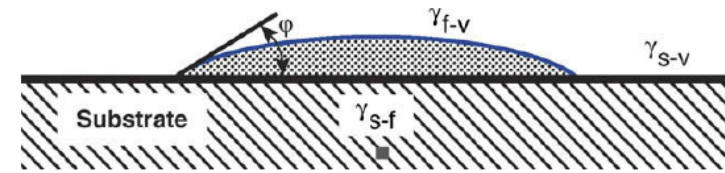


Figure 12.6: Schematic representation of a hemispherical cap-shaped island on a solid substrate. The γ terms are interfacial energies per unit area and the subscripts s, f, and v symbolize the substrate, film, and vapor phases. The wetting angle ϕ is related to the interfacial energies through Young's equation: $\gamma_{s-v} = \gamma_{f-s} + \gamma_{f-v} \cos \phi$.

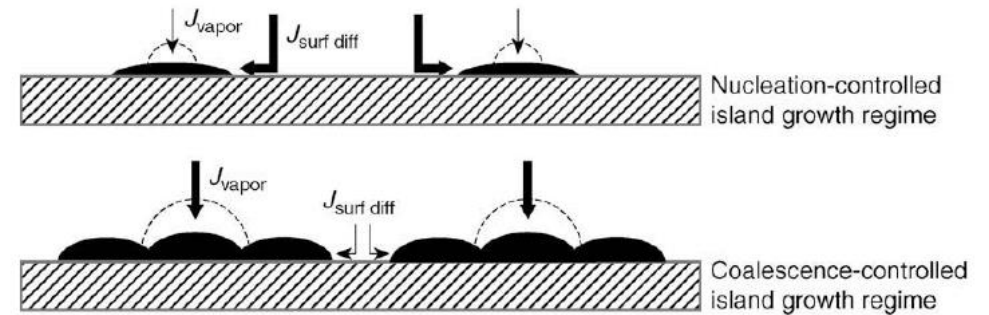


Figure 12.12: Schematic illustration of island growth in the nucleation-controlled (rate determined primarily by deposition onto the open terrace followed by surface diffusion) and coalescence-controlled (rate determined primarily by direct deposition) regimes. The dashed lines indicate equilibrium island shapes with a larger wetting angle ϕ . The widths of the arrows symbolize the magnitude of adatom supply. (Adapted from [51].)

EARLY STAGES OF GROWTH

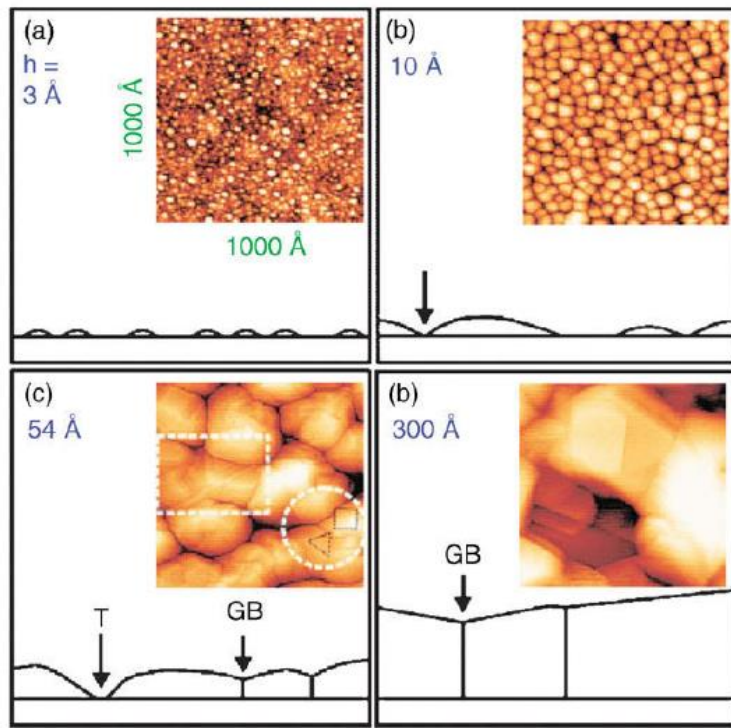


Figure 12.13: STM images ($1000 \times 1000 \text{ \AA}^2$) of Ag layers deposited by MBE on a-Si substrates to thicknesses of (a) 3, (b) 10, (c) 54, and (d) 300 \AA . The deposition rate was $R = 0.08 \text{ \AA/s}$. Schematic cross-sectional representations are also shown in which T and GB symbolize trenches and grain boundaries, respectively. (Adapted from [51].)

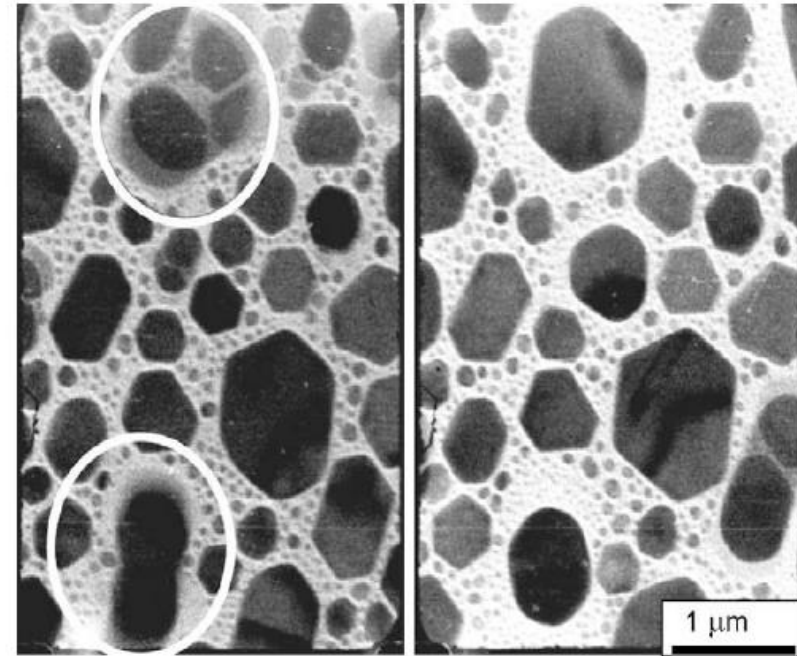
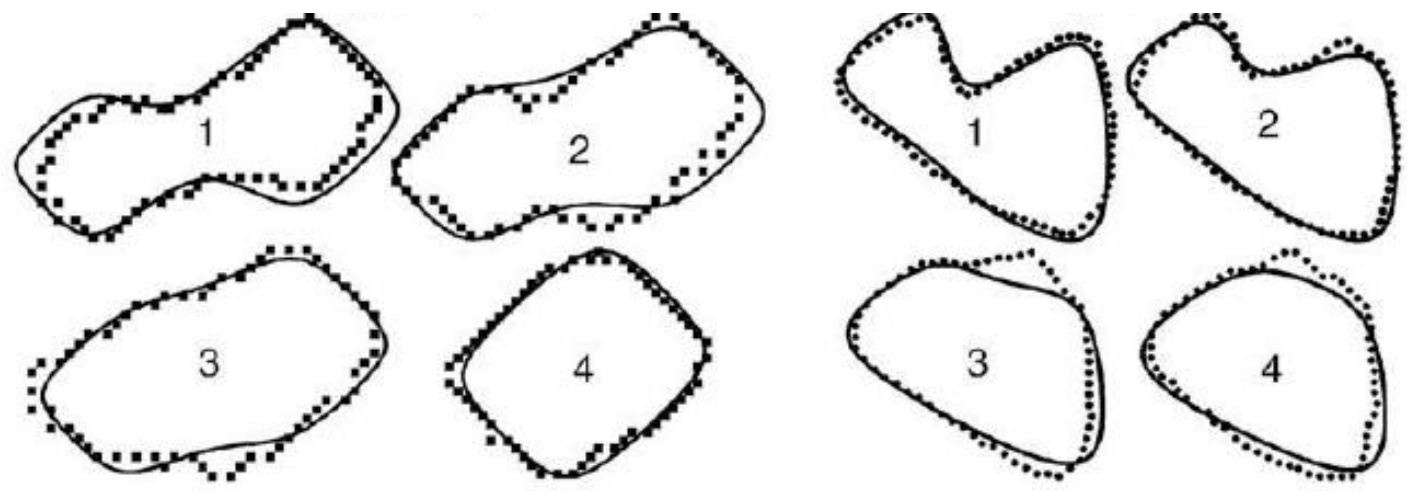
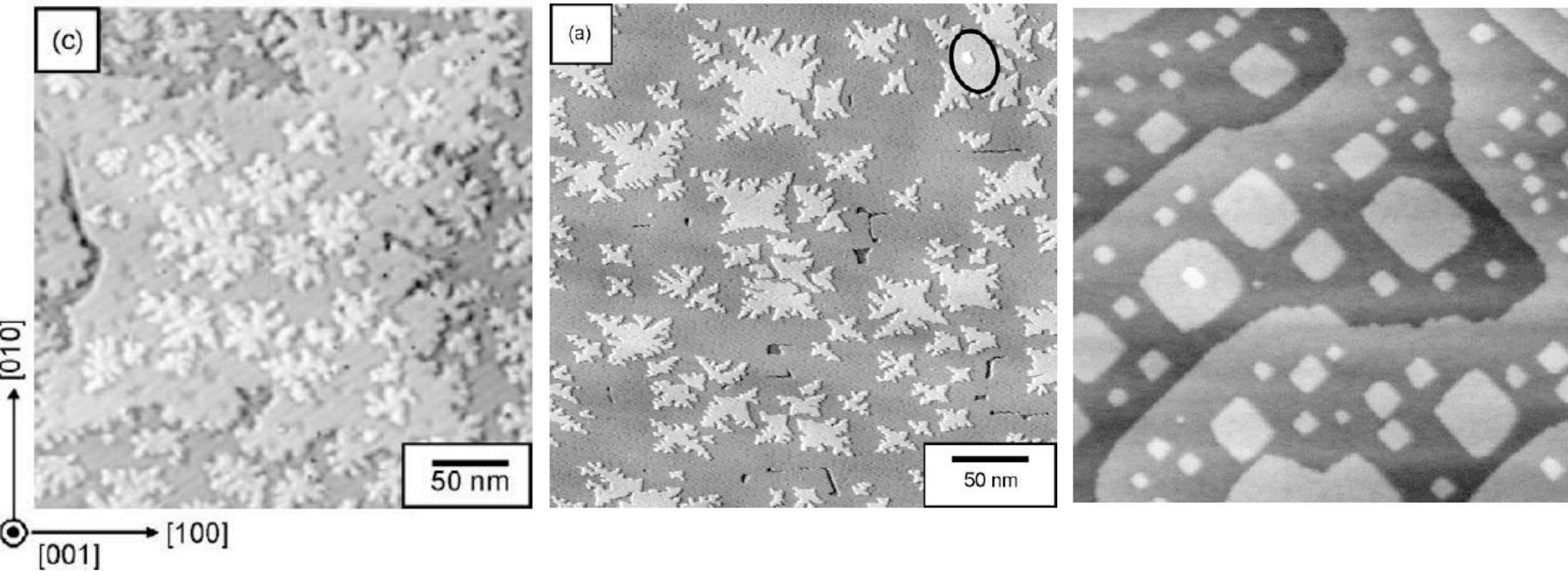


Figure 12.15: In situ plan-view TEM micrographs obtained during the growth and coalescence of In islands deposited at 5 \AA/s on amorphous C substrates at $T_s = 540 \text{ }^\circ\text{C}$. The time lapse between obtaining the left and right images is 0.3 s. Note the denuded zones surrounding the coalesced islands. (From [54].)

Depositione TiN cambiando flusso e temperatura del substrato



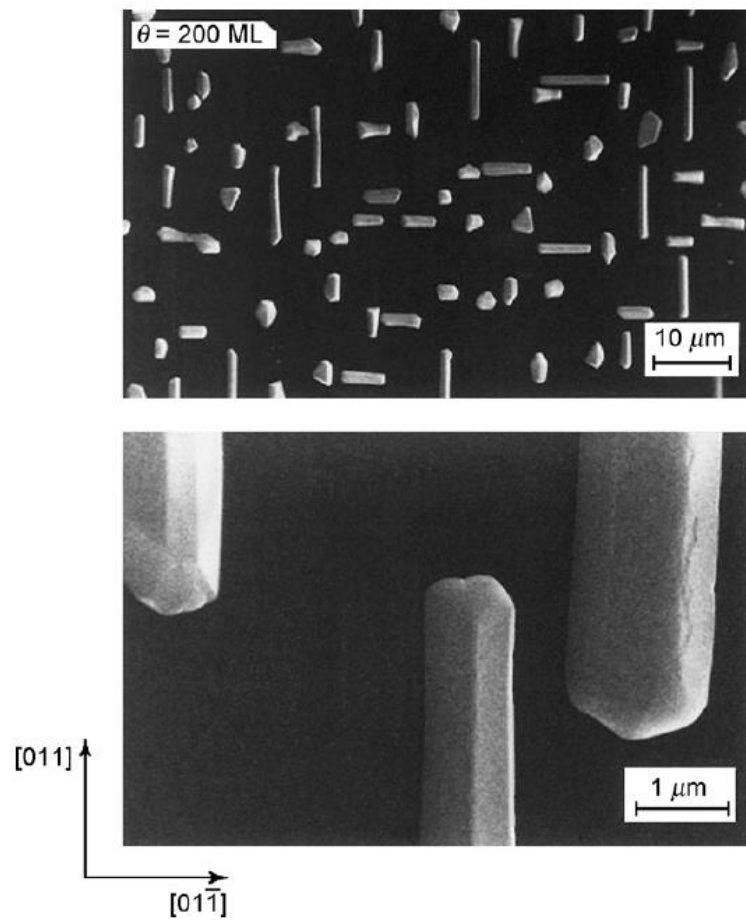


Figure 12.27: Scanning electron micrographs of polyhedral In islands on Si(001)2×1-In. The In layer was deposited by MBE with $J_{\text{In}} = 1.1 \times 10^{13} \text{ cm}^{-2} \text{ s}^{-1}$ (0.016 ML/s) at $T_s = 70^\circ \text{C}$ to a coverage $\theta_{\text{In}} = 200 \text{ ML}$. The In islands are elongated along [011] and [01 $\bar{1}$] directions and the black background is the In wetting layer. (Adapted from [20].)

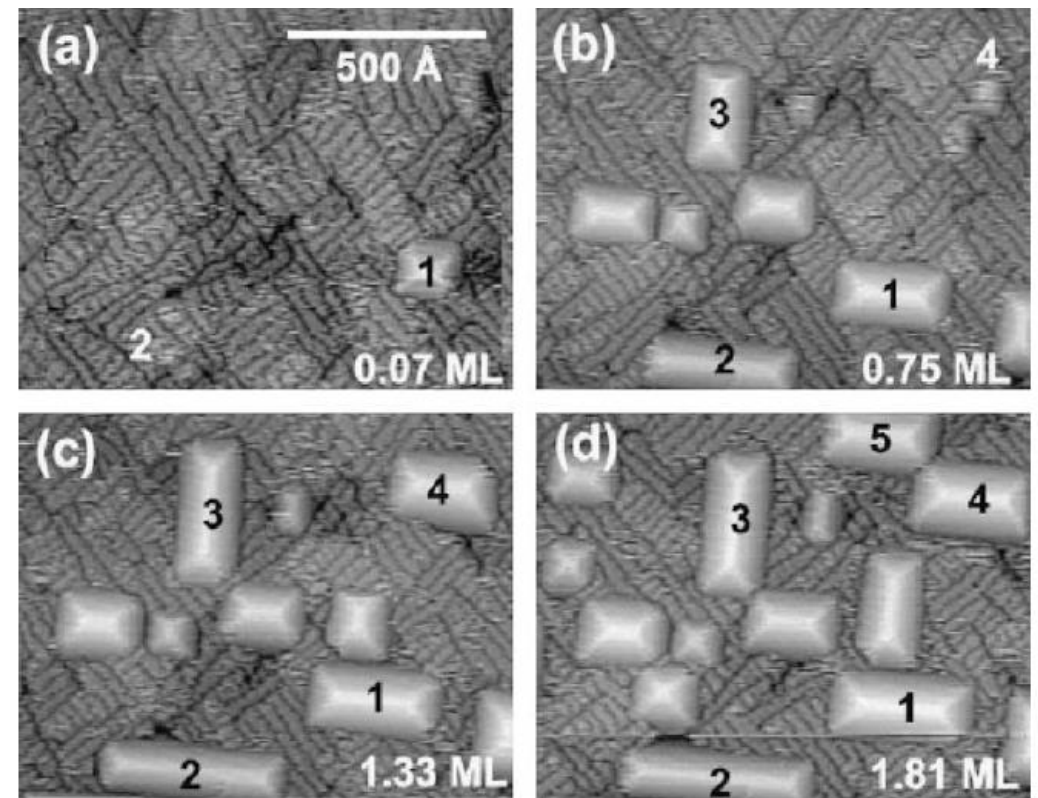
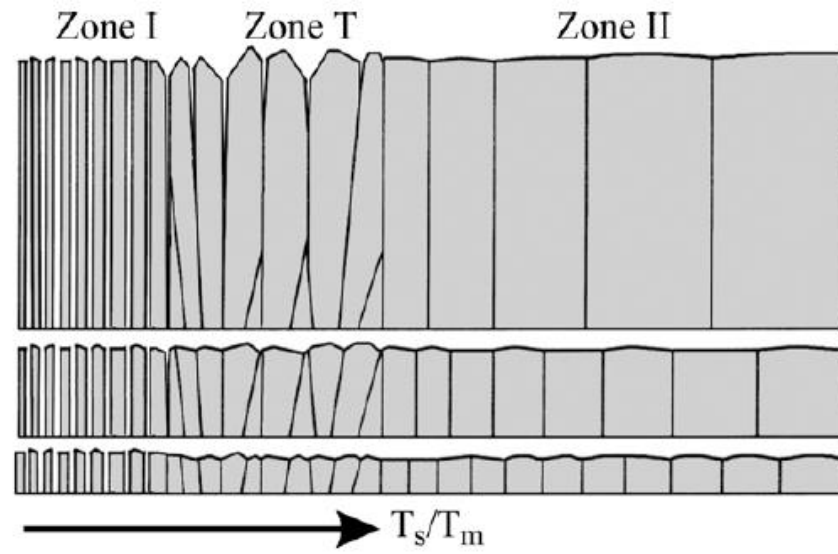
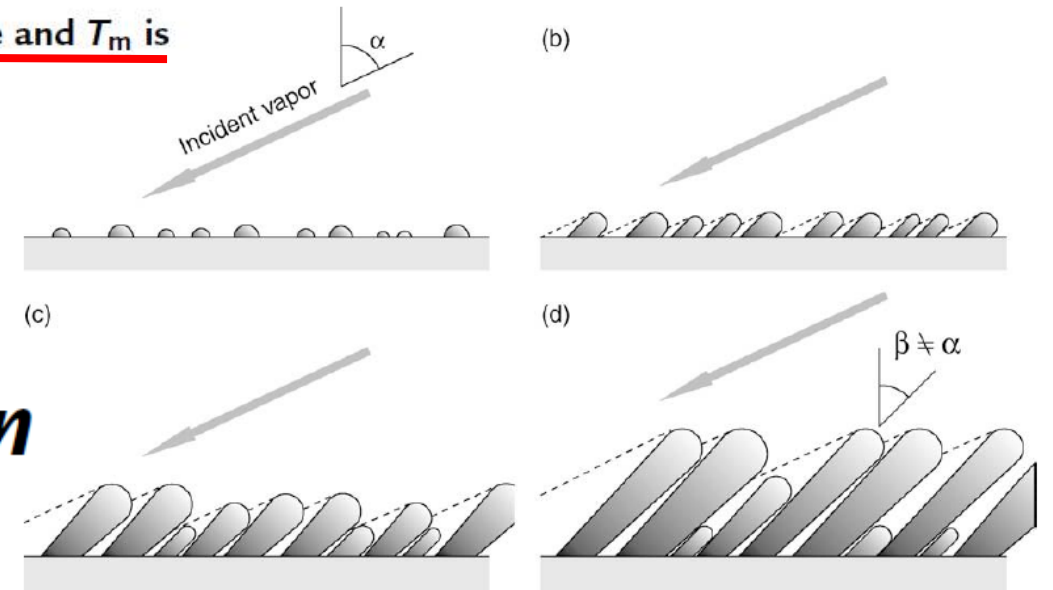


Figure 12.30: In situ STM images of MBE-grown Ge pyramids as a function of coverage (above the wetting layer) on Si(001)2×1. Image size = $1000 \times 1000 \text{ \AA}^2$, $T_s = 300^\circ \text{C}$, and $R = 0.001 \text{ ML/s}$. (From [82].)



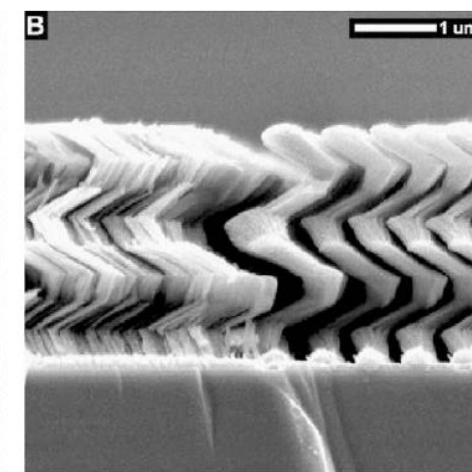
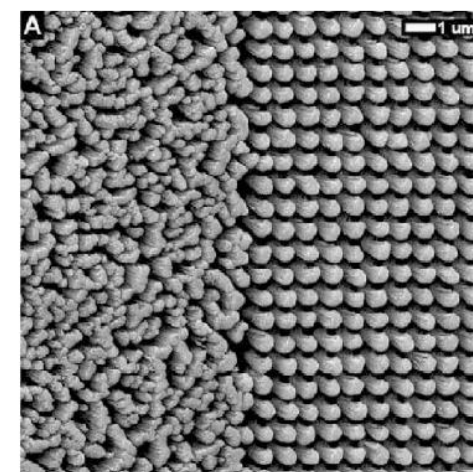
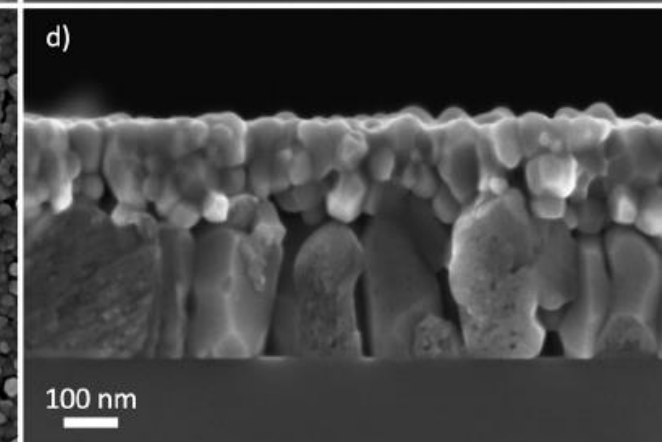
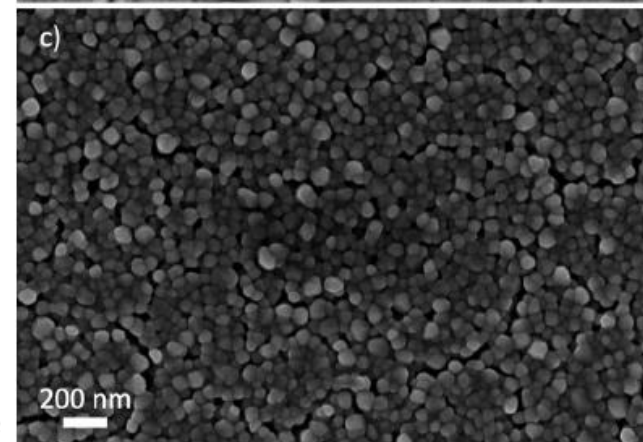
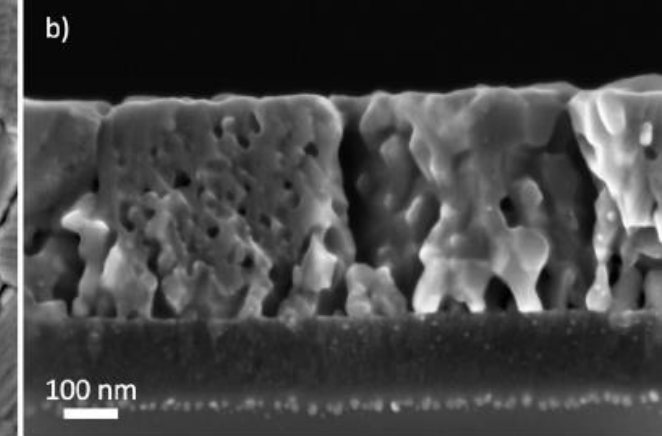
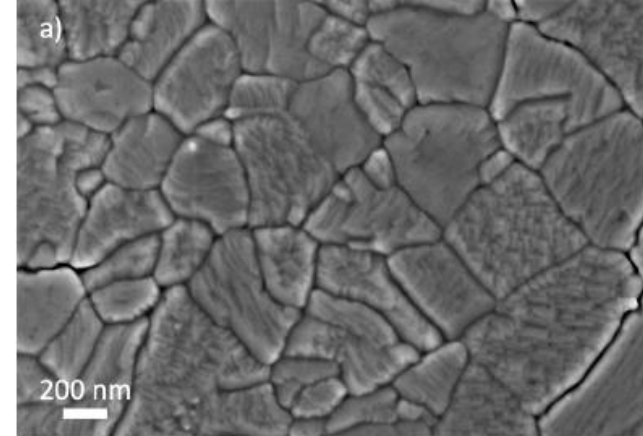
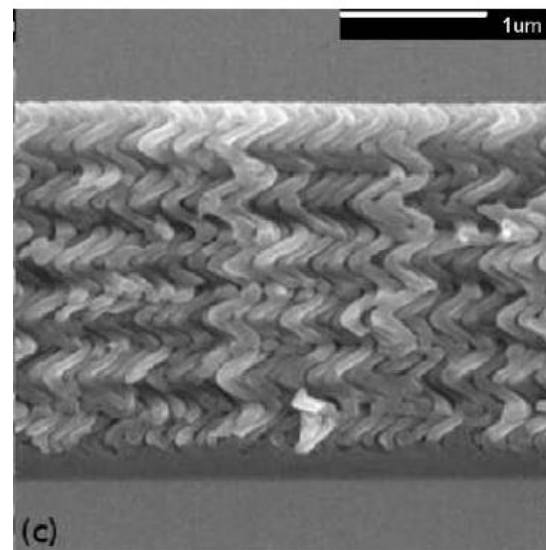
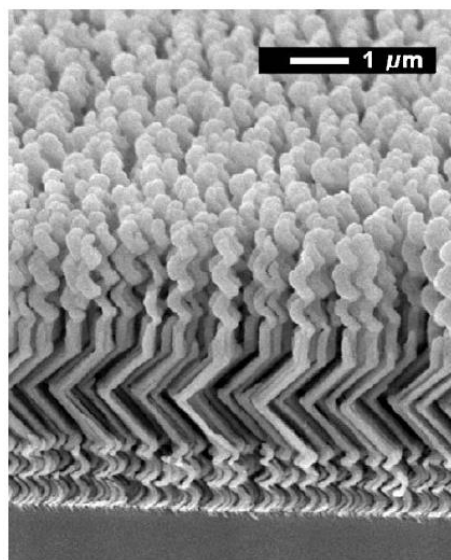
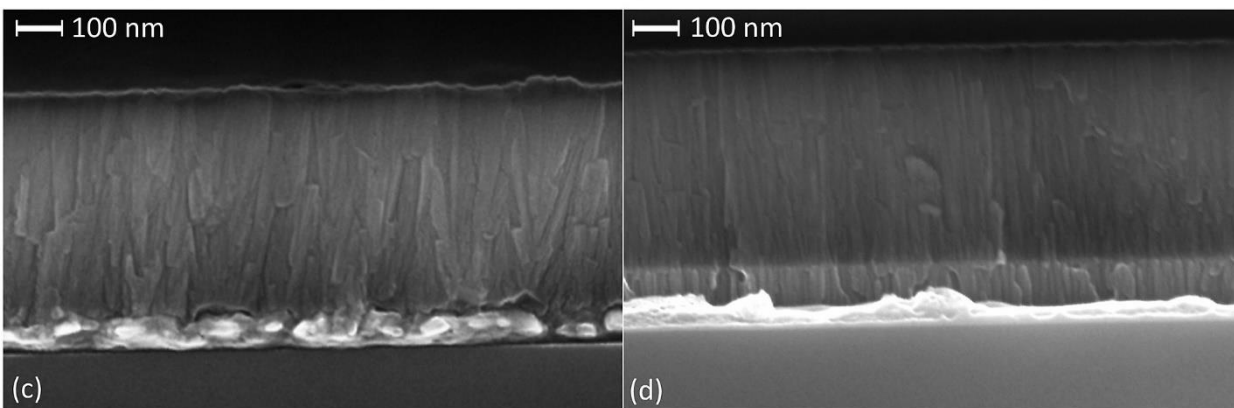
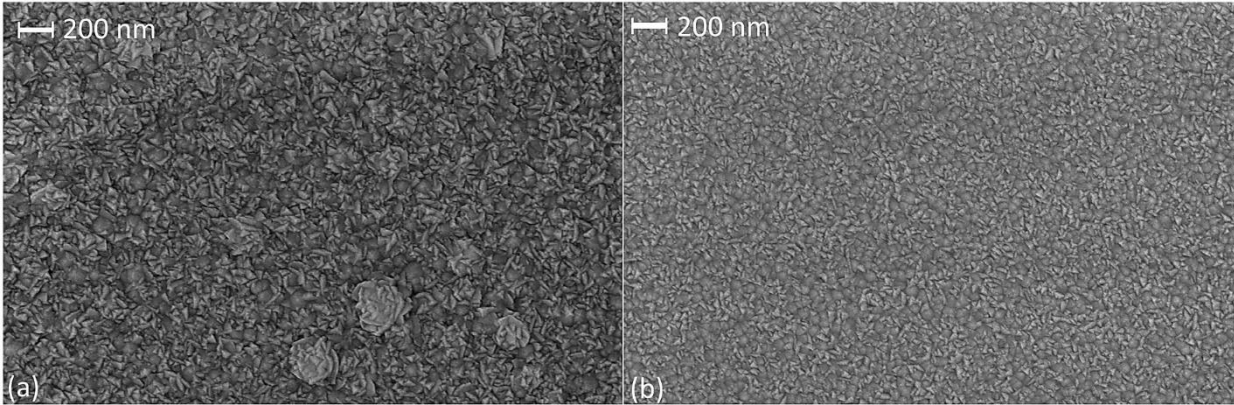
LATE STAGES OF GROWTH

Figure 12.33: SZM schematically representing microstructural evolution of pure elemental films as a function of the reduced temperature T_s/T_m , where T_s is the deposition temperature and T_m is the melting point of the material, both expressed in K. (From [8].)



Glancing Angle Deposition

Figure 13.2: Schematic view of GLAD growth: (a) initial arrival of vapor flux at an angle α , producing a random distribution of nuclei on substrate surface; (b) nuclei grow, casting shadows across substrate; (c) columns develop, partially shadowing smaller neighbors and suppressing their growth; (d) columns grow at an inclined angle $\beta \approx \alpha$. Some columns have become extinct, fully shadowed by larger neighbors. Further growth is restricted to the top of columns.



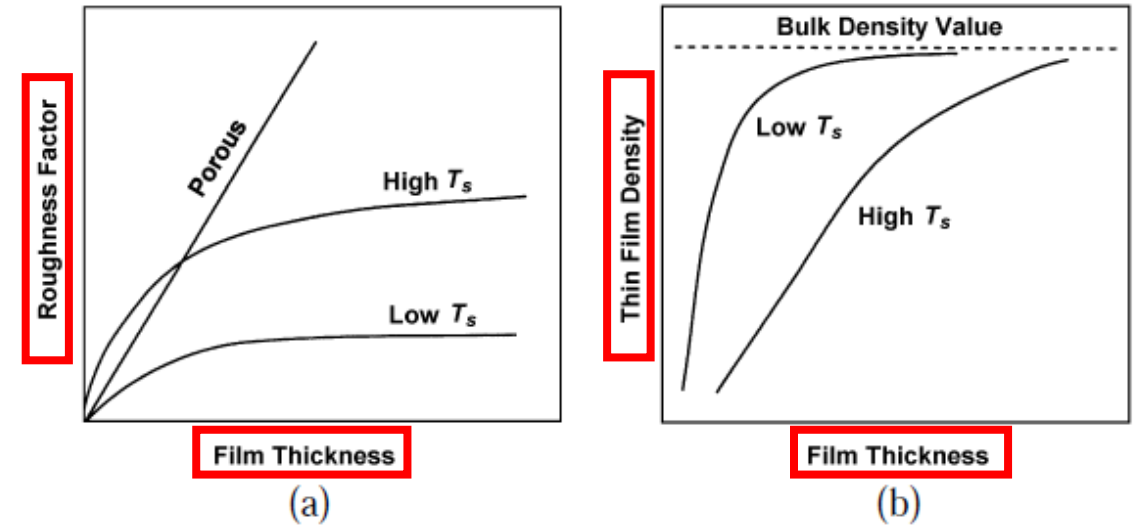
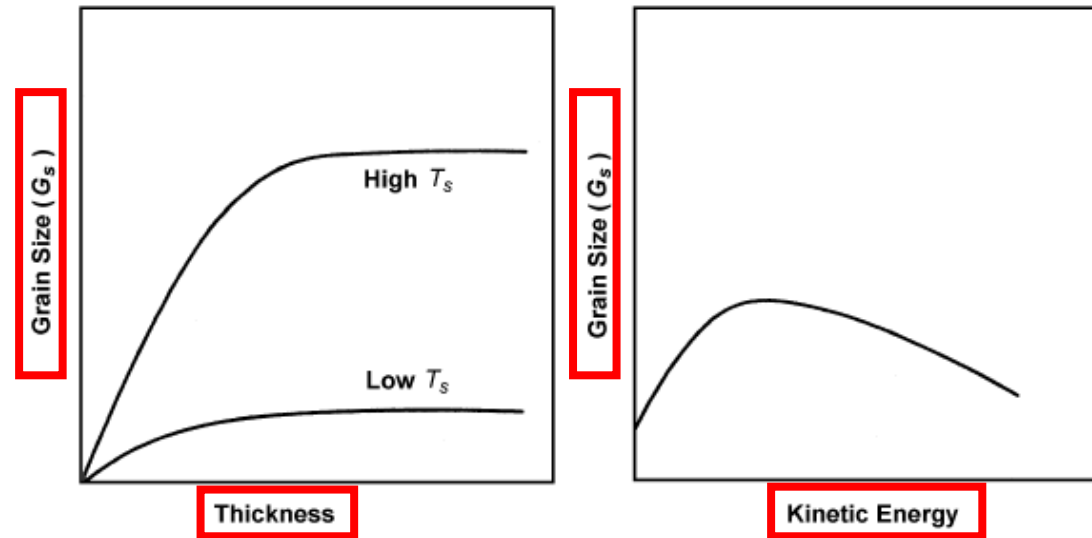
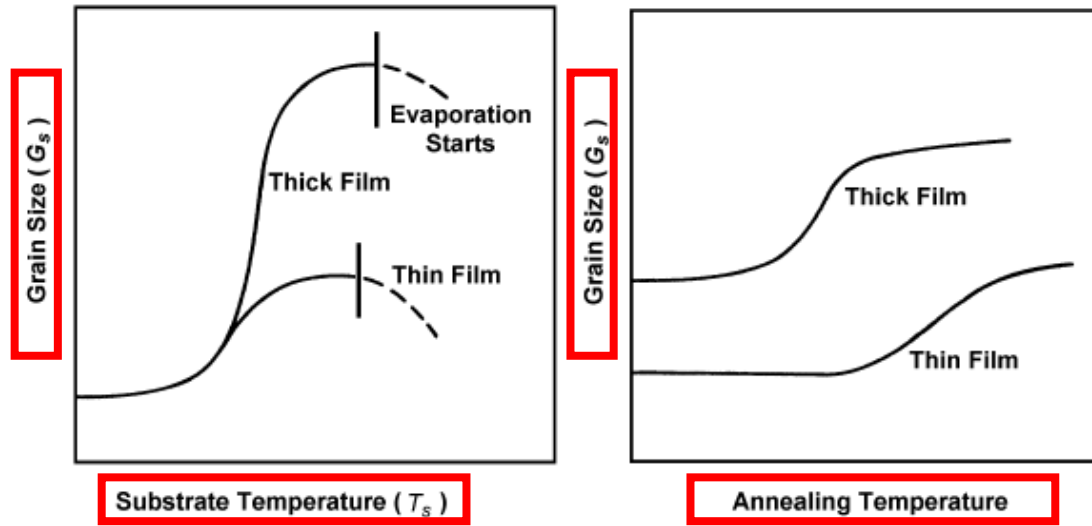


Figure 2.7. Qualitative variation of (a) the roughness factor and (b) the film density as a function of film thickness.^[2]

A quantitative measure of roughness, the *roughness factor*, is the ratio of the real effective area to the geometrical area. The roughness factor, $\Delta\theta$, is given by

Eq. (2.7)
$$\Delta\theta = \left[\theta^2 - \left(\frac{1}{N} \sum_i h_i^2 \right) \right]^{1/2}$$

Figure 2.5. Qualitative representation of the influence of various deposition parameters on the grain size of thin films.^[2]

Field	Application with examples
Engineering/ Processing	<p><i>Tribology:</i></p> <ul style="list-style-type: none">• Protective coatings to reduce wear [6, 7]• Corrosion and erosion [8]• Low friction coatings [9] <p><i>Self-supporting coatings:</i></p> <ul style="list-style-type: none">• Refractory metals for rocket nozzles [10]• Crucibles [11]• Pipes [12] <p><i>Others:</i></p> <ul style="list-style-type: none">• Hard coatings for cutting tools [13]• Surface passivation [14]• Protection against high temperature corrosion [15]• Decorative coatings [16]• Catalyzing coatings [17]

Decorative/Functional Coating

IntechnoQ

Optics

- Antireflex coatings (“multicoated optics”) [18]
- Highly reflecting coatings (laser mirrors) [19]
- Interference filters [20]
- Beam splitter and thin film polarizers [21]
- Integrated optics [22]

Optoelectronics

- Photodetectors [23]
- Image transmission [24]
- Optical memories [25]
- LCD/TFT [26]

Transparent Conductive Thin Films

Electronics	<ul style="list-style-type: none"> • Passive thin film elements [27] (resistors, condensers, interconnects) • Active thin film elements [28] (transistors, diodes) <i>Flat Panel Displays and Molecular Electronics</i> • Integrated circuits [29] (VLSI, very large-scale integrated circuit) • CCD (charge coupled device) [30]
Electricity (without semiconductors)	<ul style="list-style-type: none"> • Insulating/conducting films [31] e.g. for resistors, capacitors • Piezoelectric devices [32]
Cryotechnics	<ul style="list-style-type: none"> • Superconducting thin films, switches, memories [33] • SQUIDS (superconducting quantum interference devices) [34]
Mechanics	<ul style="list-style-type: none"> • "Hard" layers (e.g. on drill bits) [35] • Adhesion providers [36] • Friction reduction [37]

Magnetics

- Hard" discs [38]

- Video/audio tape [38]

Sensorics

- Data acquisition in aggressive environments and media [39]

- Telemetry [40]

- Biological sensorics [41]

Chemistry

- Diffusion barriers [42]

- Protection against corrosion/oxidation [43]

- Sensors for liquid/gaseous chemical [44]

Biomedicine

- Biocompatible implant coating [45]

- Neurological sensors [46]

New materials

- Metastable phases: metallic glasses [47, 48]

- Spheroidization of high melting point materials (diameter 1–500 μm) [49]

- High purity semiconductors (GaAs) [50]

(Alternative)

energies

- Solar collectors and solar cells [51]

- Thermal management of architectural performance of ETFE foils (metal-coated foils) [52]

Thin Film Solid Oxide Fuel Cells

Thin Film Solar Cells and Batteries

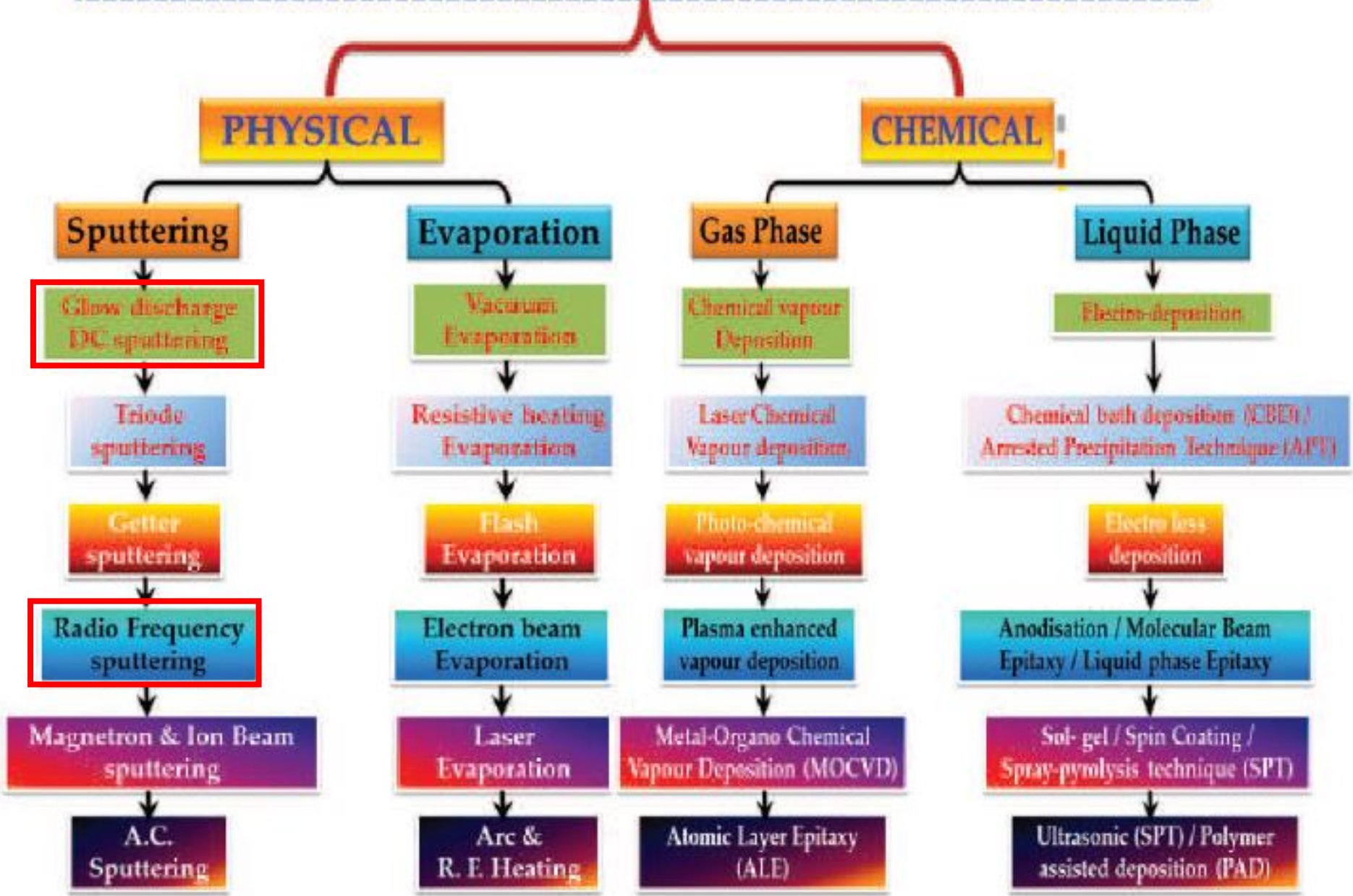
Thin film deposition is usually divided into two broad categories [3, 4].

- **Physical deposition process**
- **Chemical deposition process**

Physical deposition refers to a widespread range of technologies in that a material is released from the source and which would be deposited on a substrate using mechanical, electromechanical or the thermodynamic processes. The two most general techniques of physical vapour deposition (PVD) are evaporation and sputtering.

Chemical deposition is stated as when a volatile fluid precursor does a chemical change on a surface leaving a chemically deposited coating.

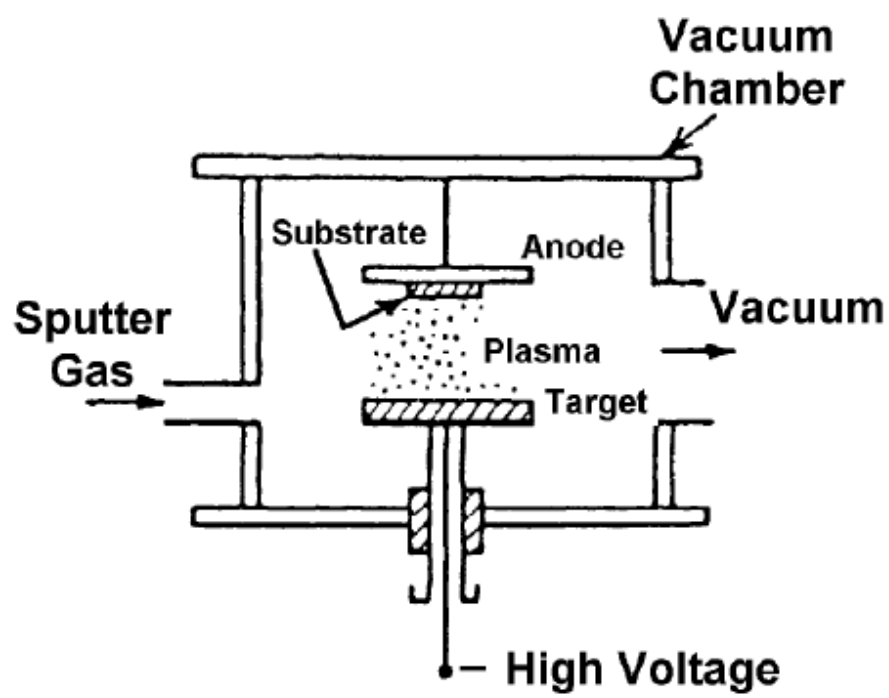
Thin Film Deposition Techniques



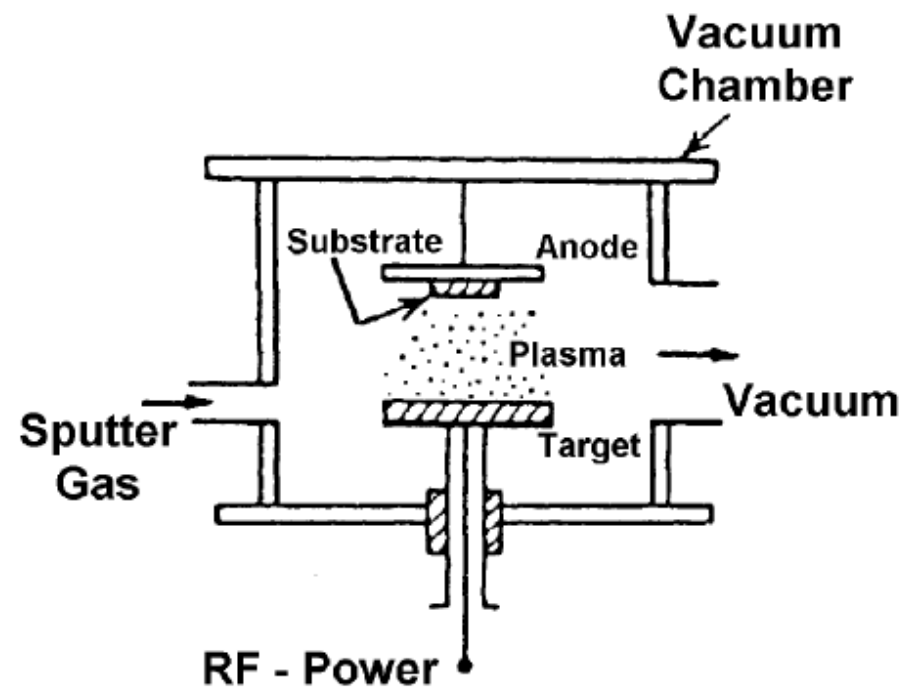
Any thin-film deposition process involves three main steps:

1. Production of the appropriate atomic, molecular, or ionic species.
2. Transport of these species to the substrate through a medium.
3. Condensation on the substrate, either directly or via a chemical and/or electrochemical reaction, to form a solid deposit.

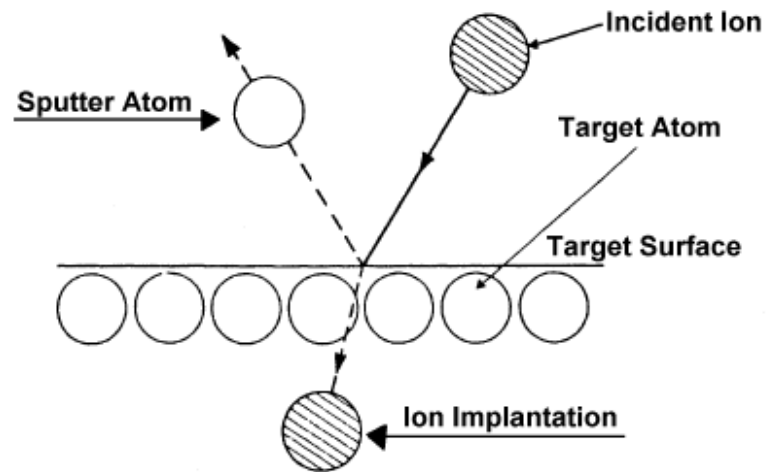
Sputter Deposition is a vacuum process which uses a different physical phenomenon to produce the microscopic spray effect. When a fast ion strikes the surface of a material (target), atoms of that material are ejected by a momentum transfer process. As with evaporation, the ejected atoms or molecules can be condensed on a substrate to form a surface coating.



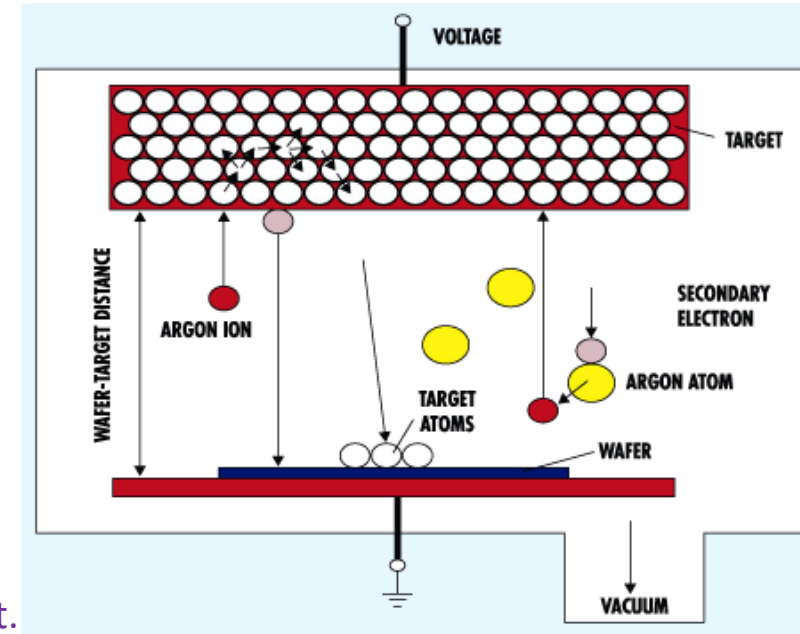
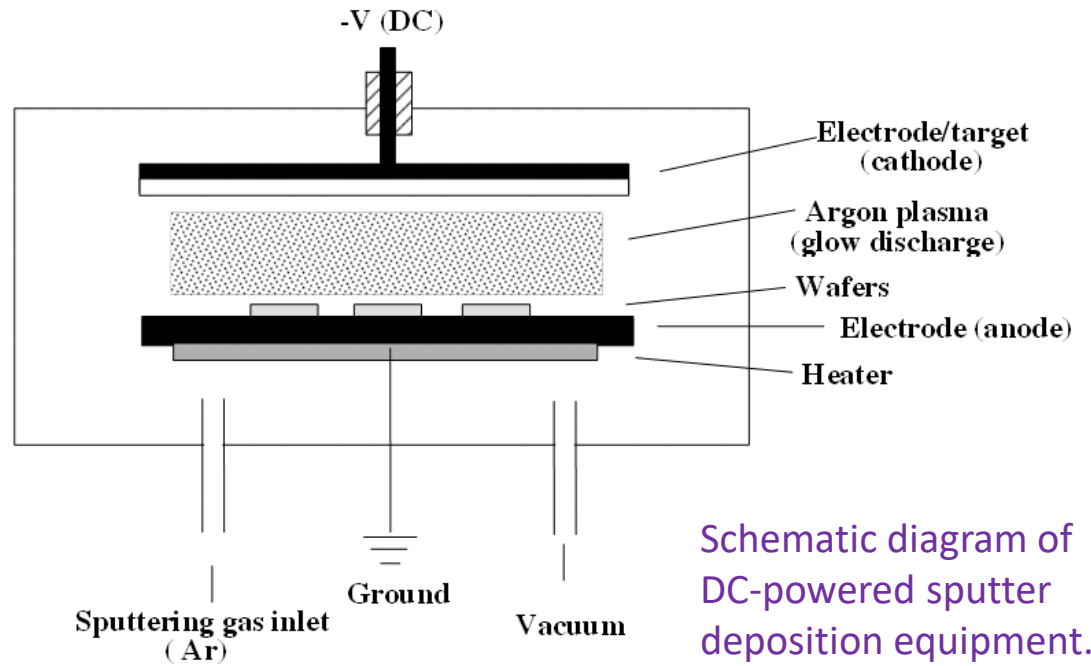
DC-Diode



RF-Diode



Sputter deposition



- Plasma is needed to make the gas conductive, and generated **ions can then be accelerated to strike the target.**
 - Higher pressures than evaporation: **1-100 mTorr.**
 - Better at depositing alloys and compounds than evaporation.
- The plasma contains \approx equal numbers of positive argon ions and electrons as well as neutral argon atoms.
Typically only $<0.01\%$ atoms are ionized!

Sputtering process

- Sputtering process can be run in **DC or RF mode (insulator must be run in RF mode)**
- Major process parameters:
 - Operation pressure (~1-100mTorr)
 - Power (few 100W)
 - For DC sputtering, voltage -2 to -5kV.
 - Additional substrate bias voltage.
 - **Substrate temperature (20-700°C)**

In addition to IC industry, a wide range of industrial products use sputtering: LCD, computer hard drives, hard coatings for tools, metals on plastics.

It is more widely used for industry than evaporator, partly because that, for evaporation:

- There are very few things (rate and substrate temperature) one can do to tailor film property.
- The step coverage is poor.
- It is not suitable for compound or alloy deposition.
- Considerable materials are deposited on chamber walls and wasted.



Targets for sputter deposition.

Sputter deposition advantages

Advantages:

- Able to deposit a wide variety of **metals, insulators, alloys and composites**.
- Replication of target composition in the deposited films.
- Capable of in-situ cleaning prior to film deposition by reversing the potential on the electrodes .
- Better film quality and step coverage than evaporation.
- This is partly because **adatoms are more energetic, and film is 'densified'** by in-situ ion bombardment, and it is easier to heat up to high T than evaporation that is in vacuum.
- More reproducible deposition control – same deposition rate for same process parameters (not true for evaporation), so easy film thickness control via time.
- **Can use large area targets** for uniform thickness over large substrates.
- Sufficient target material for many depositions.
- No x-ray damage.

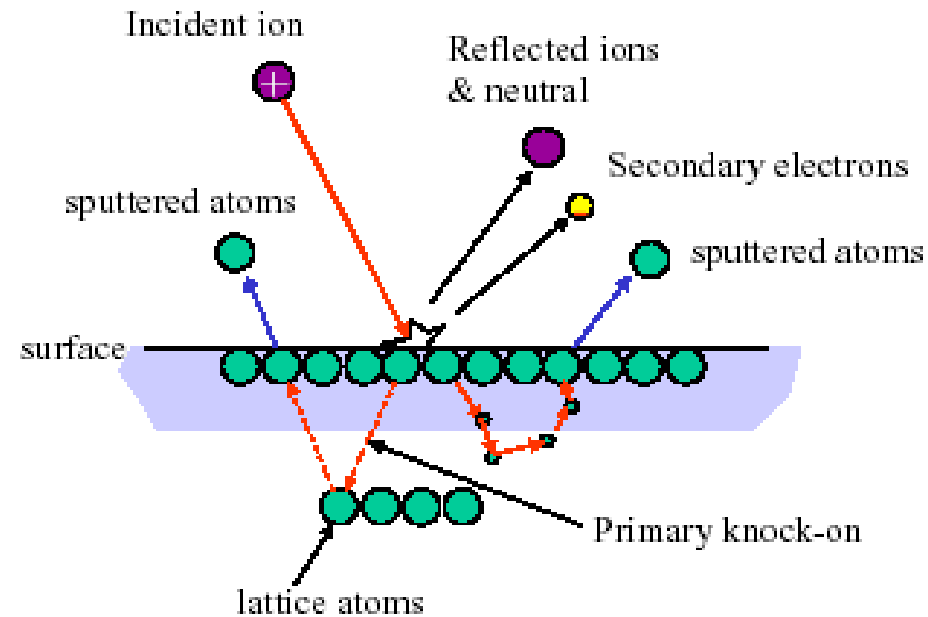
Disadvantages:

- **Substrate damage due to ion bombardment** or UV generated by plasma.
- **Higher pressures 1 –100 mtorr (< 10⁻⁵ torr in evaporation), more contaminations** unless using ultra clean gasses and ultra clean targets.
- Deposition rate of some materials quite low.
- Some materials (e.g., organics) degrade due to ionic bombardment.
- Most of the energy incident on the target becomes heat, which must be removed.

Mechanisms of sputtering and alloy sputtering

The ion impact may set up a series of collisions between atoms of the target, possibly leading to the ejection of some of these atoms. **This ejection process is known as sputtering.**

Here we are interested in sputter deposition. Of course sputter can also be used as an etching method (the substrate to be etched will be the 'target'), which is called sputter etching.

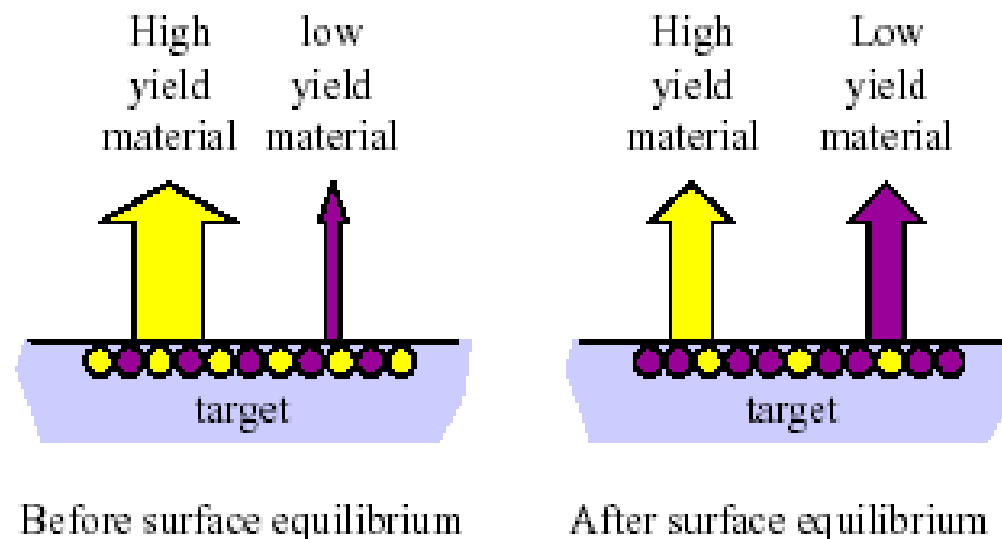


Alloys

Unlike evaporation, composition of alloy in film is approximately the same as target.

Target NOT melted, slow *diffusion* (no material flow) mixing.

When target reaches steady state, surface composition balances sputter yield.



DC plasma

Plasma is ionized gas, with nearly equal number of ions and electrons, plus neutrals (un-ionized molecules including those at ground state and excited state; free radicals such as atomic O, H, F – but no free radicals for Ar plasma).

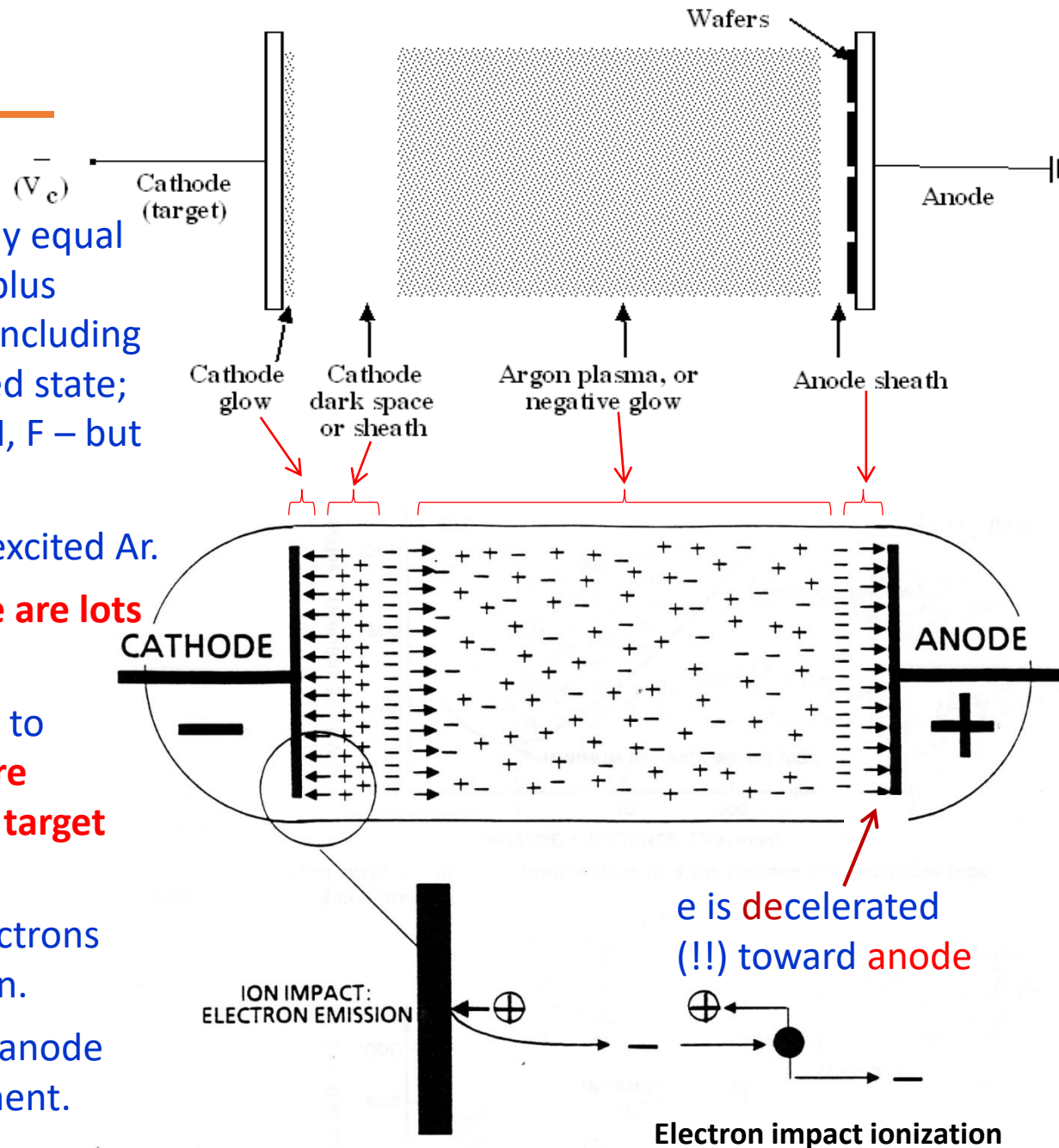
Glow is due to de-excitation of excited Ar.

So glow only exists where there are lots of electrons to excite Ar.

Cathode glow region: very close to cathode, **secondary electrons are created by Ar bombardment of target material.**

Cathode dark space/sheath: electrons pass too fast with little excitation.

Anode sheath: electrons lost to anode due to its faster *random* movement.



Explanation of DC plasma structure

Different velocities in a plasma:

Thermal energy random movement of Ar – 400 m/sec, order $(k_B T/m_{Ar})^{1/2}$.

Thermal energy random movement of electron – 10000 m/sec.

Velocity of Ar with energy 100eV – 20000 m/sec.

Velocity of electrons with energy 100eV – 6000000 m/sec.

Thus plasma is highly conducting due to fast electrons – very little voltage drop in the plasma area where electrons are rich.

Voltage drop is only possible near the electrodes where electrons may be lost to the electrode.

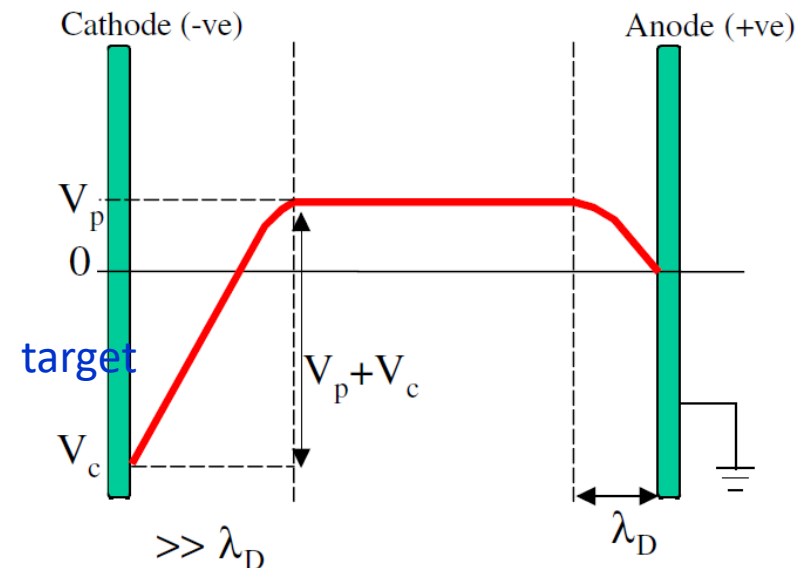
Even without applied voltage (assume plasma still exist), voltage drop may still exist due to faster *random* electrons movement that leads to their loss to electrode.

Therefore, the plasma is always positively biased relative to any electrode or anything (floating or not) inside the plasma.

This positive bias will accelerate positive Ar ion to strike the electrode.

But the bias V_p near the anode is very small ($\sim 10V$), so no significant sputtering of the substrate.

The total bias (V_p plus applied voltage) is very high, leading to sputtering of cathode (target).



Sputtering process

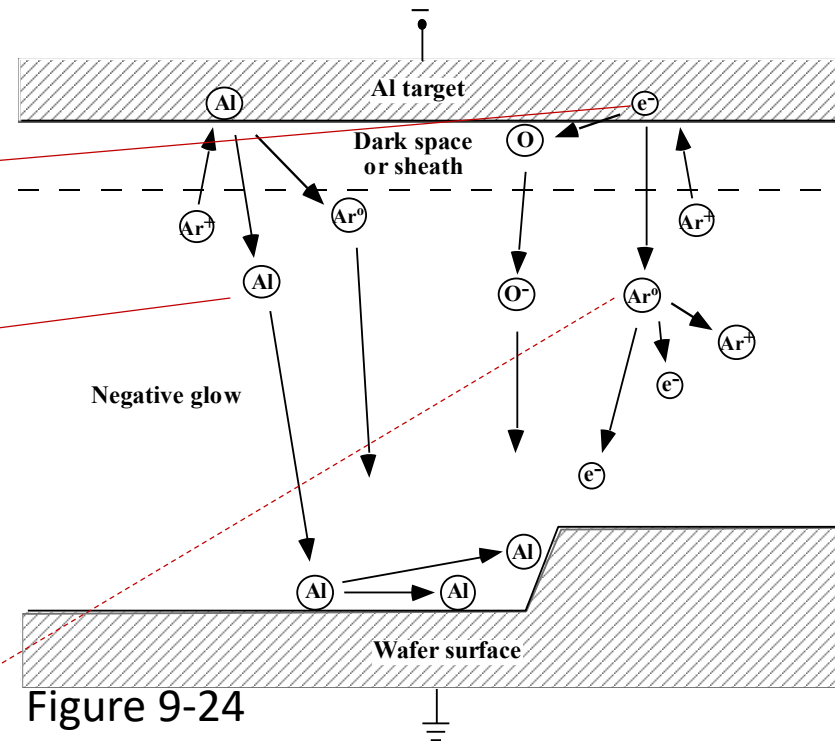
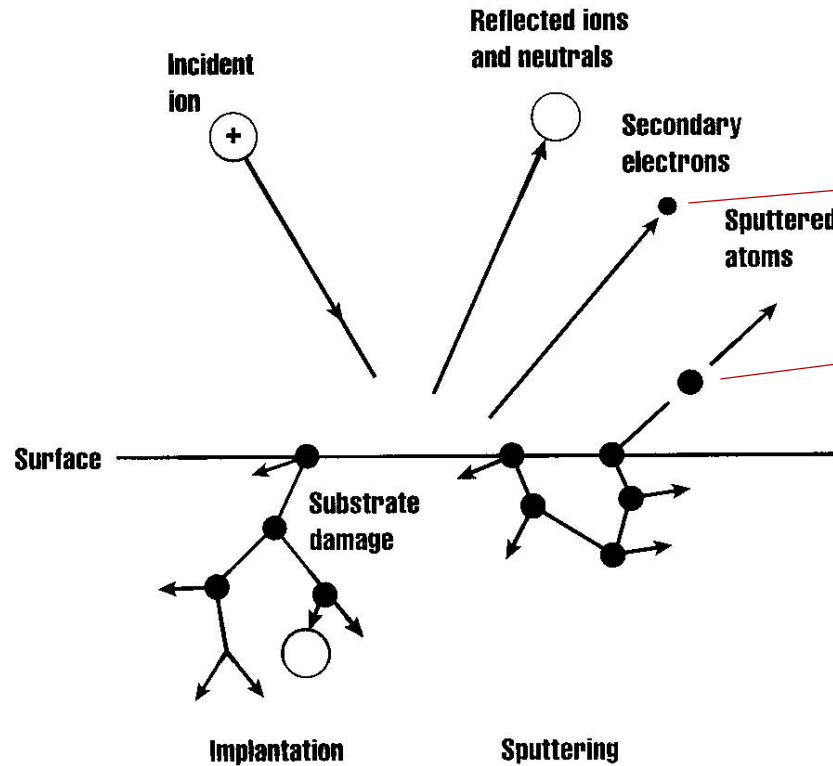


Figure 9-24

After collision ionization, there are now TWO free electrons. This doubles the available electrons for ionization.

This ongoing doubling process is called "impact ionization", which sustains a plasma.

On the left side, sputter off an Al atom. On the right side, generate secondary electrons, which are accelerated across the sheath region and 1) ionize/excite an Ar; or 2) ionize an impurity atom, here O, to generate O^- (for Ar, always positive ion Ar^+). This O^- is accelerated toward substrate and may go into the film (bad).

Sputtering process

- **Energy of each incoming ion is 500-1000eV. Energy of sputtered atoms is 3-10eV.**
- Thus, the sputtering process is very inefficient from the energy point of view, 95% of incoming energy goes to target heating & secondary electron.
- **High rate sputter processes need efficient cooling techniques to avoid target damage from overheating** (serious problem).
- The sputtered species, in general, are predominantly neutral.
- The energy of the ejected atoms shows a Maxwellian distribution with a long tail toward higher energies.
- **The energies of the atoms or molecules sputtered at a given rate are about one order of magnitude higher than those thermally evaporated at the same rate, which often lead to better film quality.**
- **However, since sputtering yields are low and the ion currents are limited, sputter-deposition rates are invariably one to two orders of magnitude lower compared to thermal evaporation rates under normal conditions.**

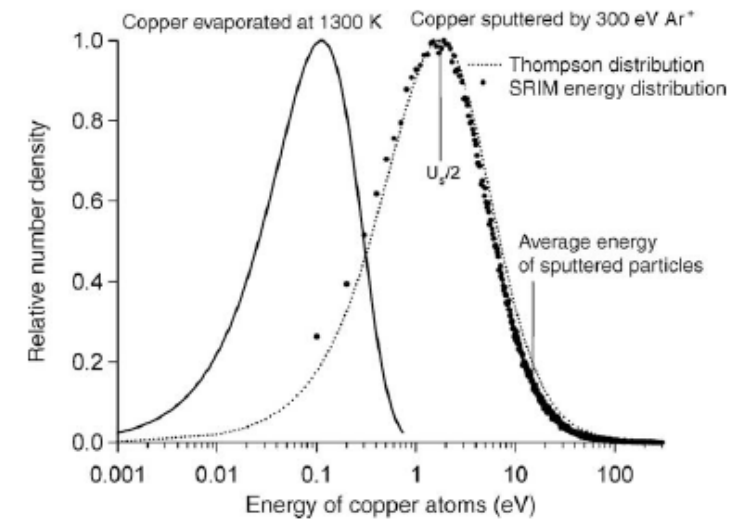
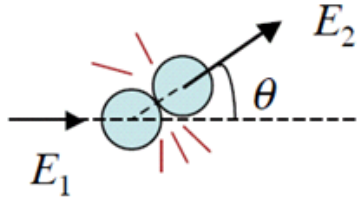


Figure 5.4: Comparison between the thermal energy distribution for copper evaporated at 1300 K and the energy distribution of sputtered copper atoms.

Sputtering yield

Elastic energy transfer



$$\frac{E_2}{E_1} \propto \frac{4M_1M_2}{(M_1 + M_2)^2} \cos^2 \theta$$

E_2 is greatest for $M_1=M_2$.

There is also inelastic energy transfer, which leads to secondary electrons emission...

$$Y = \frac{\text{sputtered atoms}}{\text{bombing ions}} = \alpha \frac{Mm}{(M+m)^2} \frac{E_m}{U_M}$$

M : mass of target atom

m : mass of bombing ion

E_m : kinetic energy of bombing ion

U_M : Bonding energy of target metal

α : depends on striking /incident angle

- Sputter yield Y : the number of sputtered atoms per impinging ion.
- Obviously, the higher yield, the higher sputter deposition rate.
- **Sputter yield is 1-3: not too much difference for different materials.**
- **The sputter yield depends on: (a) the energy of the incident ions; (b) the masses of the ions and target atoms; (c) the binding energy of atoms in the solid; and (d) the incident angle of ions.**
- The yield is rather insensitive to the target temperature except at very high temperatures where it show an apparent rapid increase due to the accompanying thermal evaporation.

Dependence of sputter yield on ion energy

A threshold energy for the release of an atom from the target exists, below which the atom is not “sputtered”.

This threshold energy is:

$$E_{threshold} = \frac{\text{Heat of Vaporization}}{\gamma(1-\gamma)}$$
$$\text{where } \gamma = \frac{4M_1M_2}{(M_1 + M_2)^2}$$

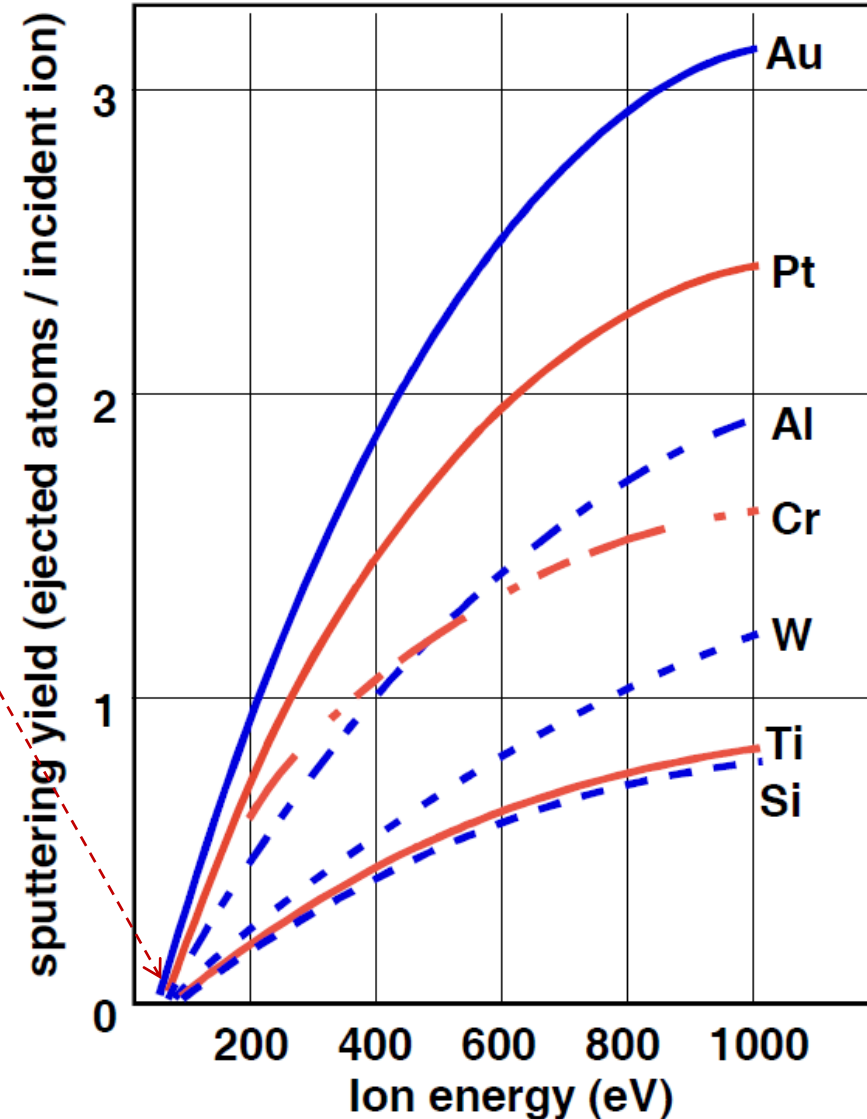
(E_{th} very high when $M_1 \approx M_2$ or they are very different?)

The yield increases with the energy.

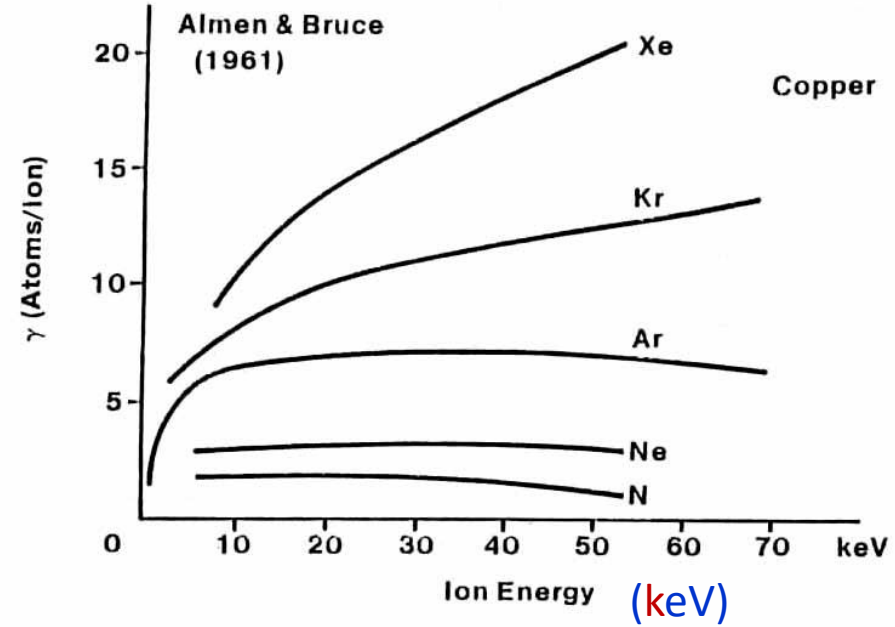
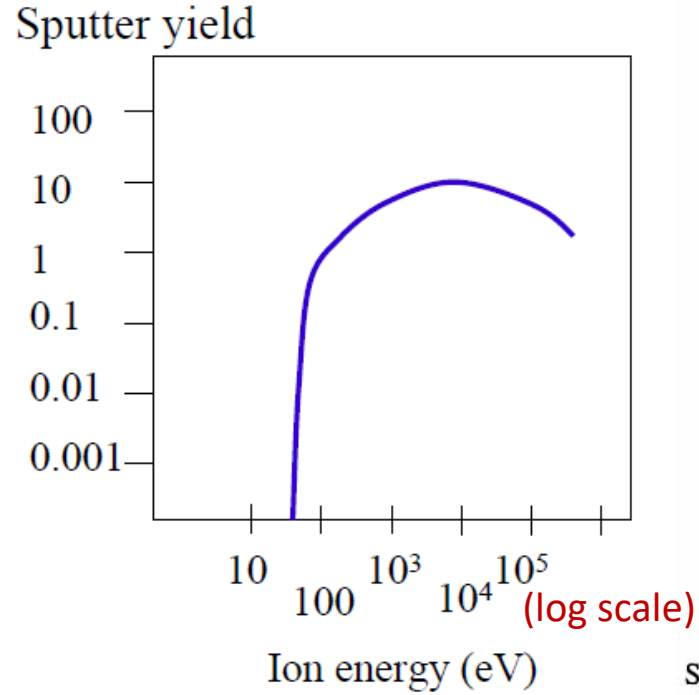
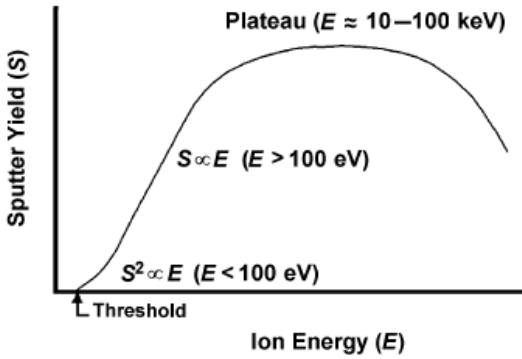
For higher energies, the yield approaches **saturation**, which occurs at higher energies for heavier bombarding particles.

e.g.: $Xe^+ \sim 100keV$ and $Ar^+ \sim 20KeV$ for saturation.

Sometimes, at very high energies, the yield decreases because of the increasing penetration depth and hence increasing energy loss below the surface, i.e. not all the affected atoms are able to reach the surface to escape.



Dependence of sputter yield on ion energy



Sputtering yields of the noble gases on copper, as a function of energy.

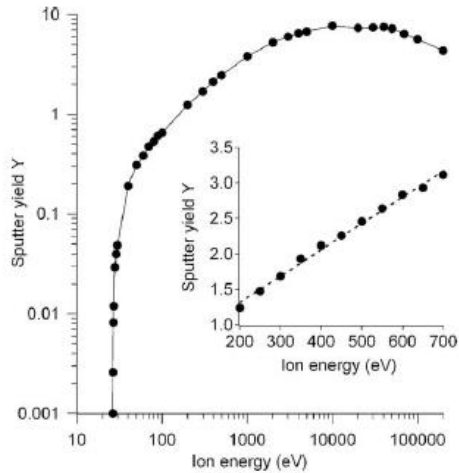
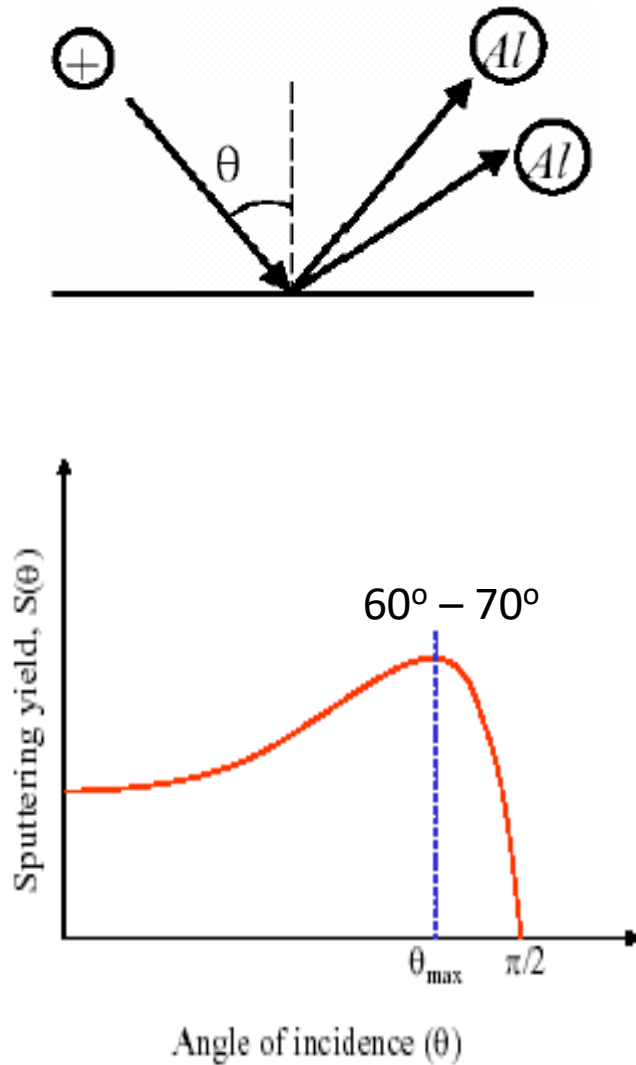


Table 11-2 SPUTTER YIELDS FOR METALS IN ARGON (ATOMS/ION)

Target	At.Wt./Dens.	100 eV	300 eV	600 eV	1000 eV	2000 eV
Al	10.0	0.11	0.65	1.2	1.9	2.0
Au	10.2	0.32	1.65	2.8	3.6	5.6
Cu	7.09	0.5	1.6	2.3	3.2	4.3
Ni	6.6	0.28	0.95	1.5	2.1	
Pt	9.12	0.2	0.75	1.6		
Si	12.05	0.07	0.31	0.5	0.6	0.9
Ta	10.9	0.1	0.4	0.6	0.9	
Ti	10.62	0.08	0.33	0.41	0.7	
W	14.06	0.12	0.41	0.75		

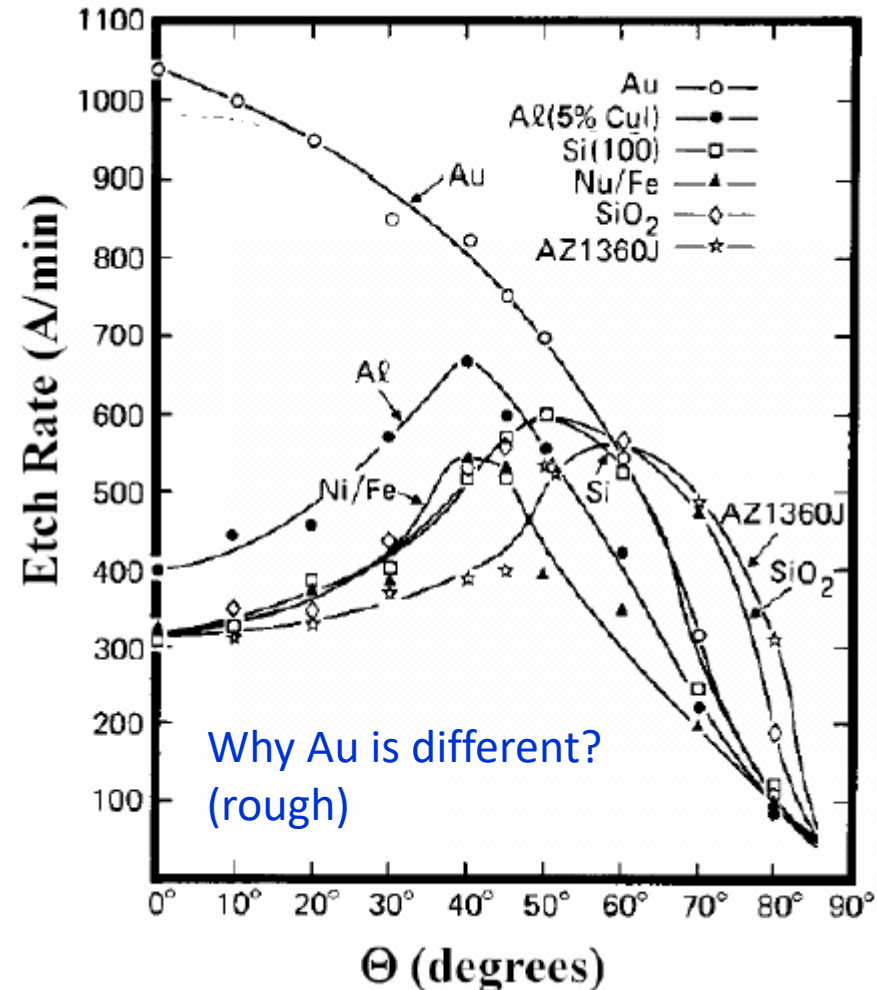
Figure 5.2: Sputtering yield Y of Cu as a function of the energy of Ar^+ at normal incidence as calculated using the SRIM code. Note that $Y(E_{\text{Ar}^+})$ is linear over the typical range of operation during magnetron sputtering ($E_{\text{Ar}^+} = 250-750$ eV).

Dependence of sputter yield on ion incident angle



The yield increases as $(\cos\theta)^{-1}$ with increasing obliqueness (θ) of the incident ions.

However, at large angles of incidence the surface penetration effect decrease the yield drastically.

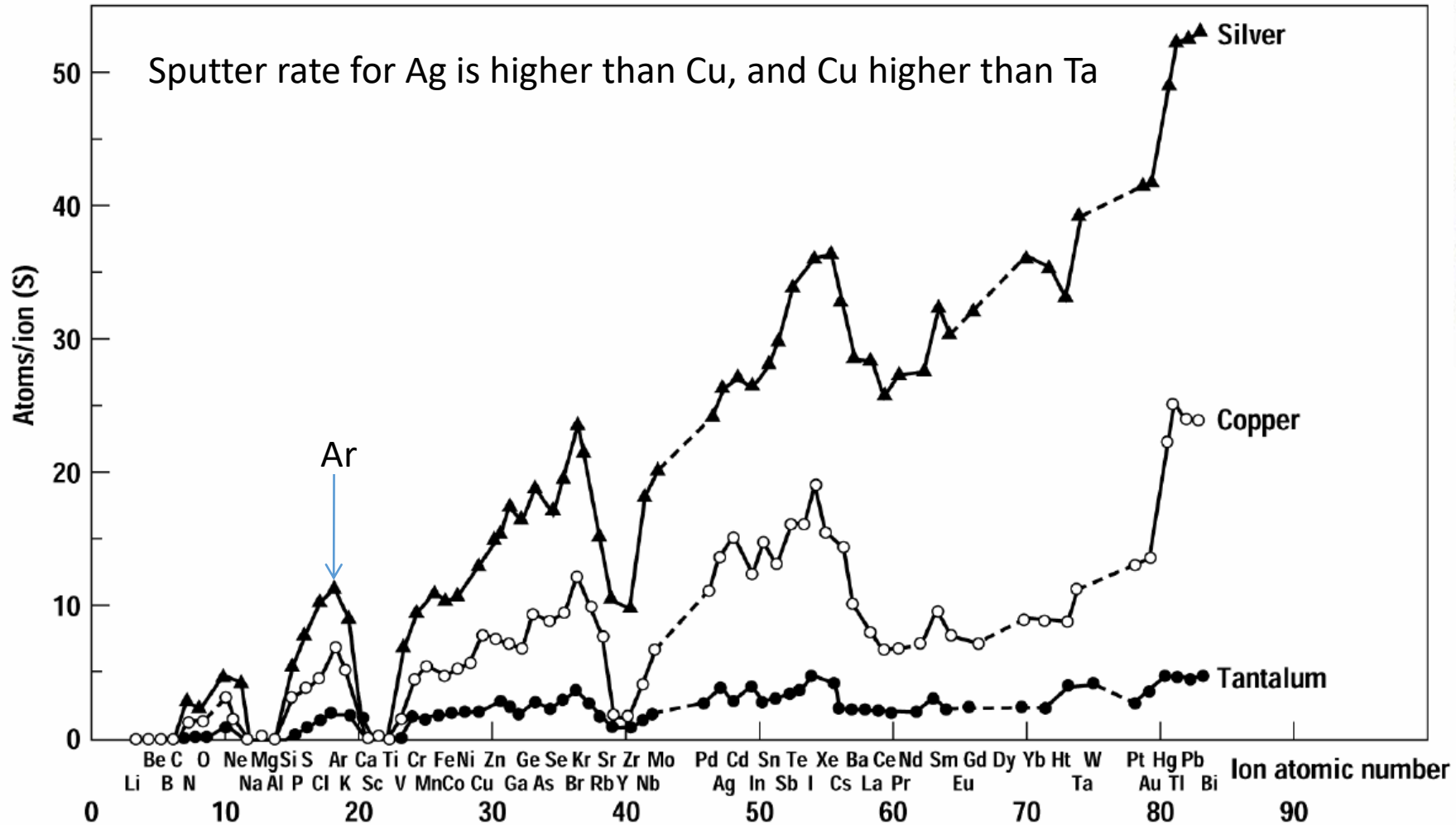


Dependence of sputter yield on ion mass

Sputter Yield increases with ion mass.

Sputter yield is a maximum for ions with full valence shells: noble gasses such as Ar, Kr, Xe have large yields.

Sputter yield of elements at 500eV



Gas	He	Ne	Ar	Kr	Xe
Element					
Be	0.24	0.42	0.51	0.48	0.35
C	0.07	—	0.12	0.13	0.17
Al	0.16	0.73	1.05	0.96	0.82
Si	0.13	0.48	0.50	0.50	0.42
Ti	0.07	0.43	0.51	0.48	0.43
V	0.06	0.48	0.65	0.62	0.63
Cr	0.17	0.99	1.18	1.39	1.55
Cu	0.24	1.80	2.35	2.35	2.05
Fe	0.15	0.88	1.10	1.07	1.00
Ni	0.16	1.10	1.45	1.30	1.22
Nb	0.03	0.33	0.60	0.55	0.53
Mo	0.03	0.48	0.80	0.87	0.87
Pd	0.13	1.15	2.08	2.22	2.23
Ag	0.20	1.77	3.12	3.27	3.32
Ta	0.01	0.28	0.57	0.87	0.88
W	0.01	0.28	0.57	0.91	1.01
Re	0.01	0.37	0.87	1.25	—
Os	0.01	0.37	0.87	1.27	1.33
Ir	0.01	0.43	1.01	1.35	1.56
Pt	0.03	0.63	1.40	1.82	1.93
Au	0.07	1.08	2.40	3.06	3.01
Au	0.10	1.3	2.5	—	7.7
Pb	1.1	—	2.7	—	—

Dependence of deposition rate on chamber pressure

Higher chamber pressure:

Mean-free path of an atom $\lambda=4.8\times 10^{-3}/P(\text{torr})$ (cm). E.g. $\lambda\sim 0.1\text{cm}$ for $P=50\text{mTorr}$.

Therefore, as typically target-substrate separation is many cm, sputtered atoms have to go through tens of collisions before reaching the substrate.

This reduces deposition rate – considerable materials are deposited onto chamber walls.

Too many collisions also prevent ionization (reduce ion density and deposition rate).

Lower chamber pressure:

(For same power) higher ion energy that increases sputter yield/deposition rate.

But **fewer Ar ions to bombard the target for deposition**, which reduces deposition rate.

Therefore, there exist an optimum pressure (provided that such a pressure can sustain the plasma) for maximum deposition rate.

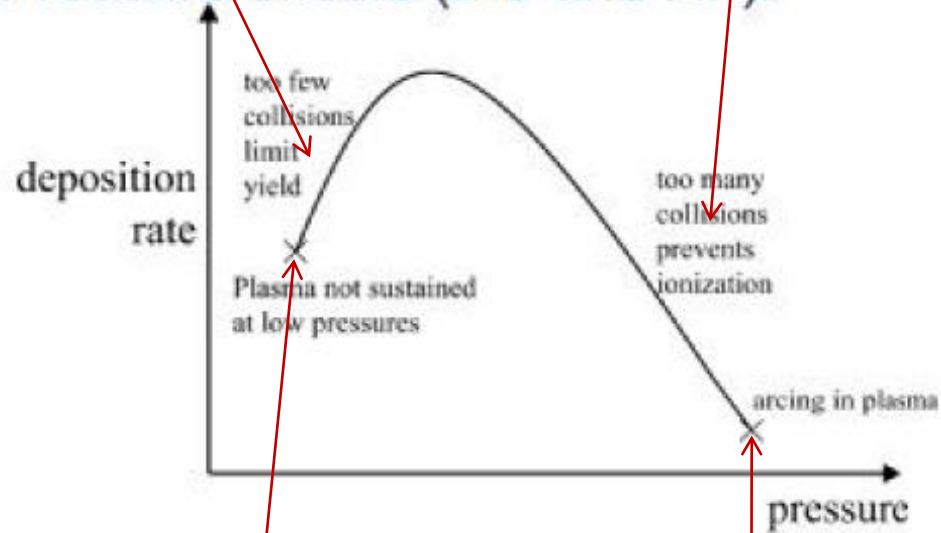
This optimum pressure depends on target-substrate configurations (their separation, target/substrate size...).

Dependence of deposition rate on chamber pressure

Too few collisions limit yield

Too many collisions prevent ionization

Pressure effects (DC and RF):



Plasma not sustained at low pressure

Arcing in plasma (?)

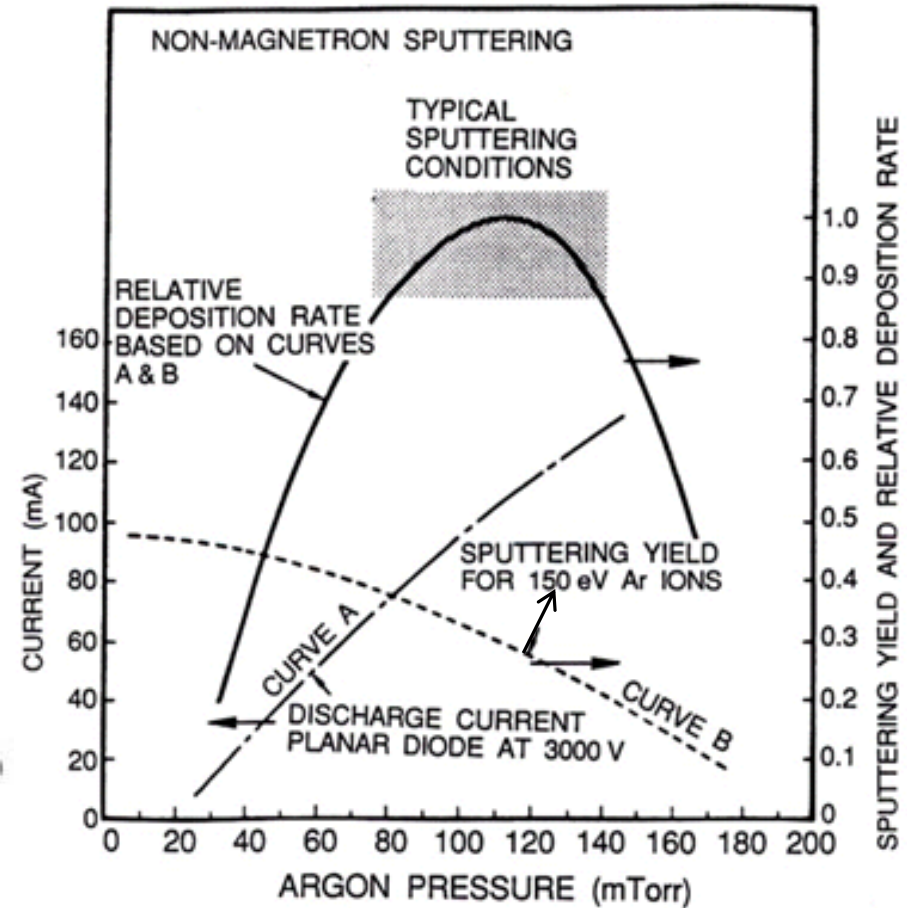


Figure 3-18 Influence of working pressure and current on deposition rate for non-magnetron sputtering.

For same power $P=I \times V = \text{constant}$, high current (ion number) comes with low voltage (ion energy)

Step coverage of sputtering

Sputtering targets are generally large and provide a wide range of arrival angles in contrast to a point source. Step coverage is mainly determined by arrival angle distribution.

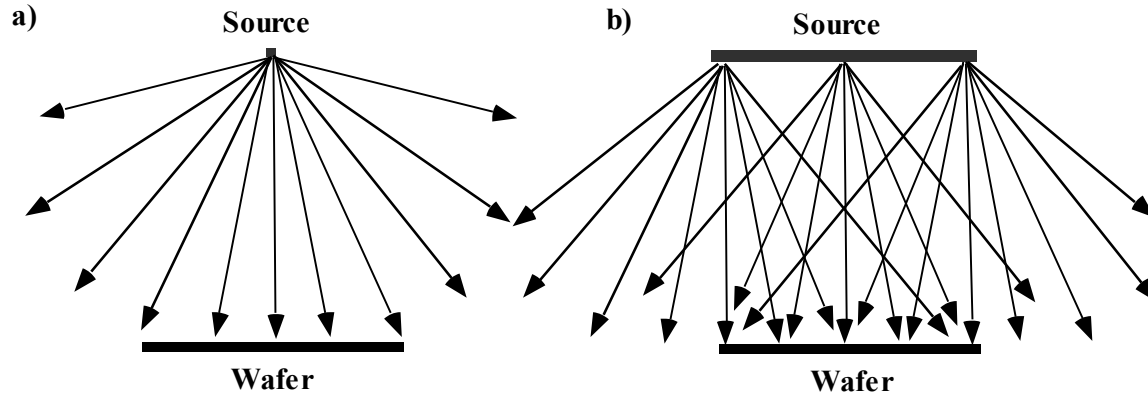


Figure 9-26

(a) Small source, wide emitted angle distribution, but a narrow arrival angle distribution.

(b) Wider arrival angle distribution.

a) Isotropic flux arrival
 $n = 1$ in $\cos^n\theta$ arrival angle distribution

b) Anisotropic flux arrival
 $n > 1$ in $\cos^n\theta$ arrival angle distribution

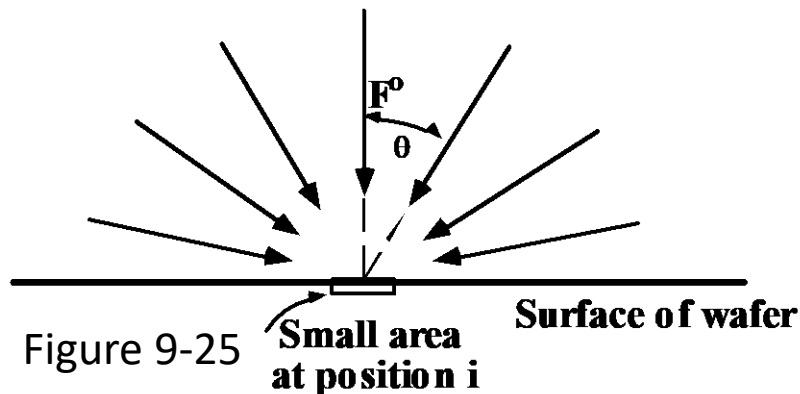
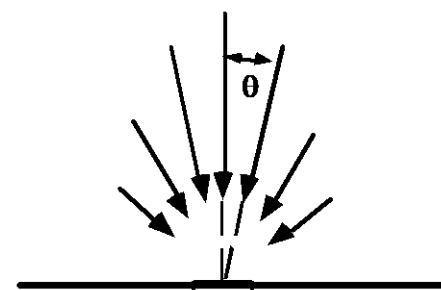


Figure 9-25

Small area at position i

Surface of wafer

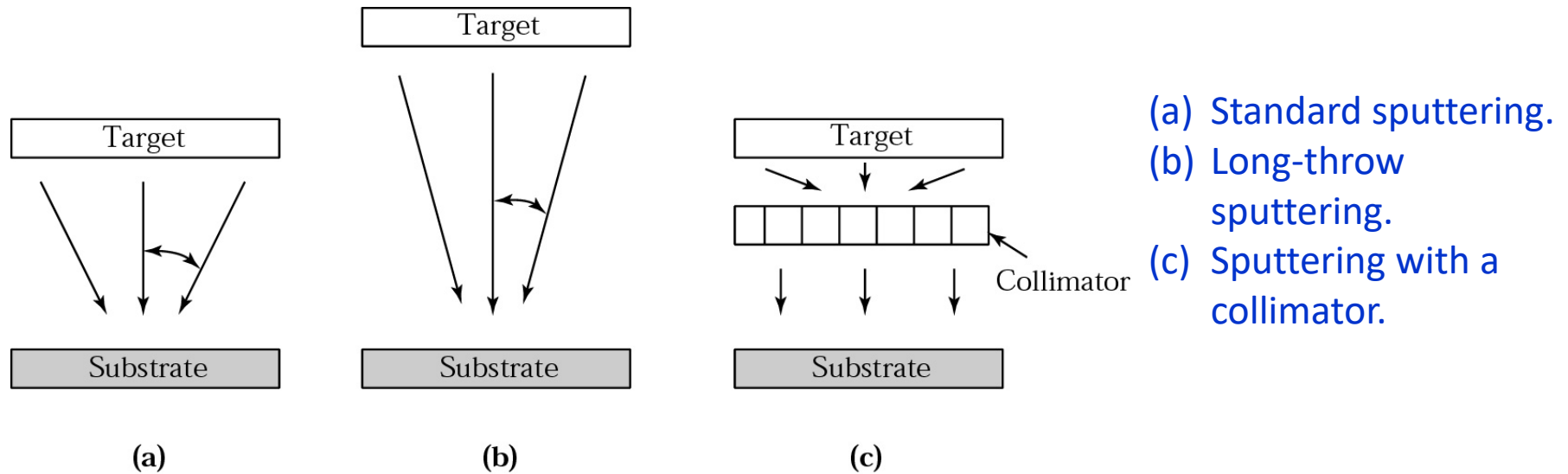


Arrival angle distribution is defined by arrival flux relative to unit surface area. The flux is equal to the *normal* component of incoming flux.

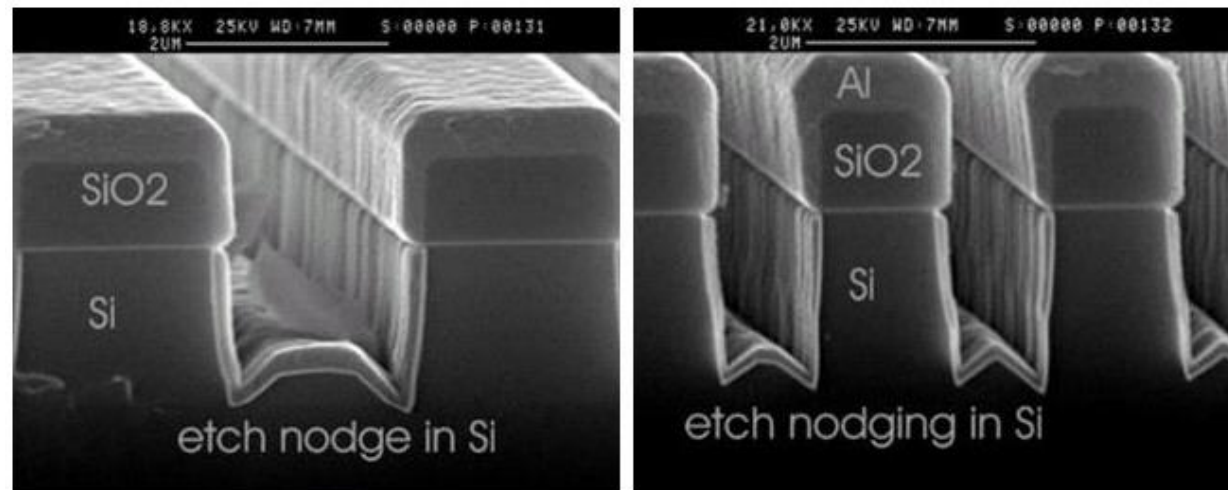
Arrival angle distribution is generally described by $\cos^n\theta$ distribution.

Size of source, system geometry and collisions in gas phase are important in arrival angle distribution.

Arrival angle can be tailored to some degree



However, when the mean free path of the *target* atom (determined by gas pressure, order 10cm for 1mTorr pressure/1cm for 10mTorr) is much shorter than target-substrate separation, many collisions will occur, which broaden the arrival angle distribution.



More deposition on top surface.

Atom migration along surface also important

- Atoms ejected from cathode escape with energies of 10 to 50 eV, which is 10-100 times the energy of evaporated atoms.
- This additional energy (together with bombardment by other ions) provides sputtered atoms with additional surface mobility for improved step coverage relative to evaporation.

(This additional energy also makes the deposited film “denser” - better film quality than evaporated film).

Besides tilting and rotating substrate, step coverage can be further improved by:

- **Substrate heating:** improve step coverage due to surface diffusion, but may produce unacceptably large grains.
- Apply bias to wafers: increase bombardment by energetic ions, but it will also sputter the deposited material off the film and thus reduce deposition rate.

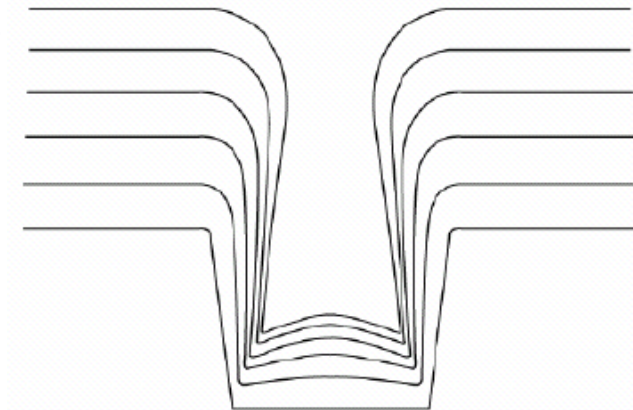
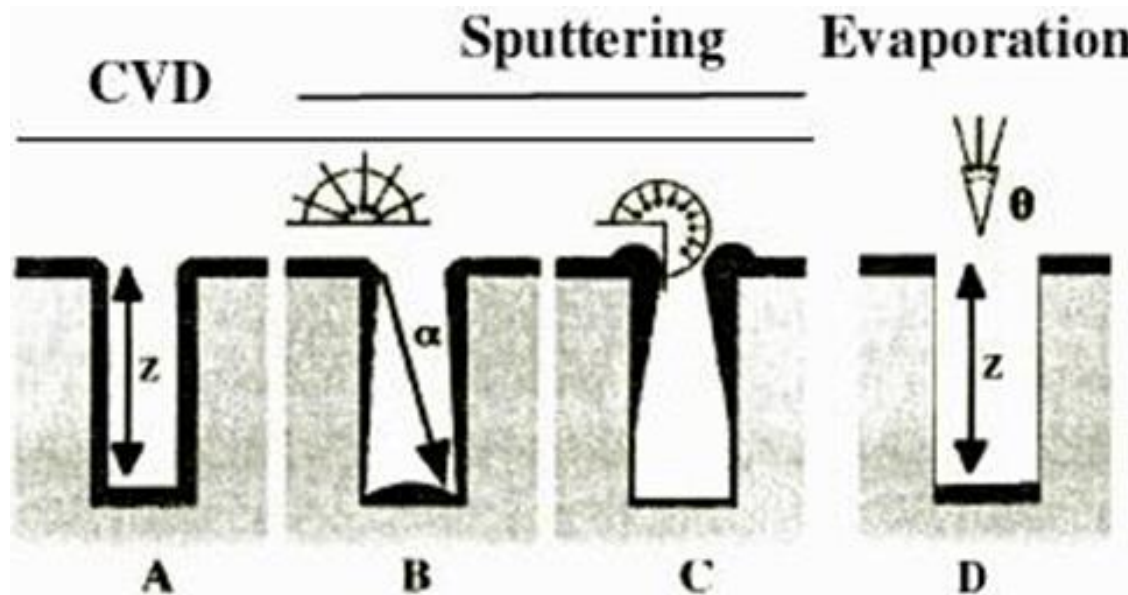
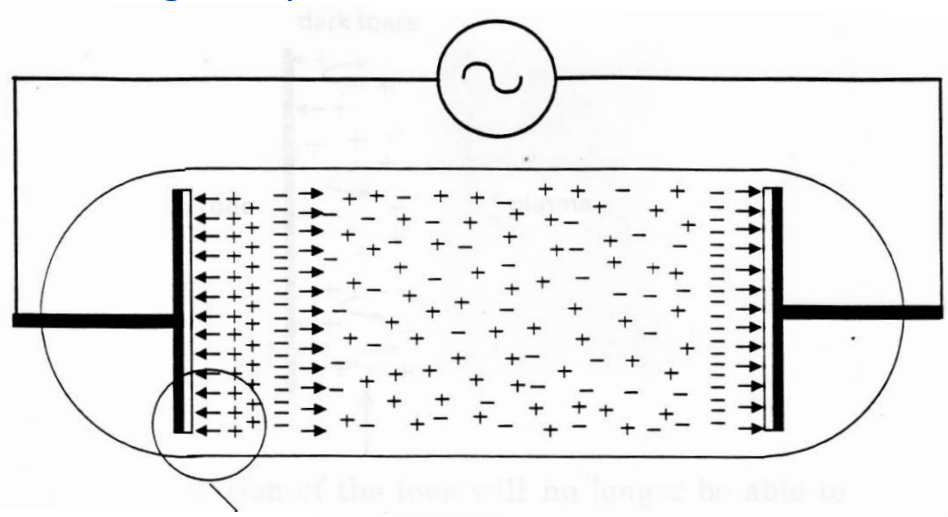


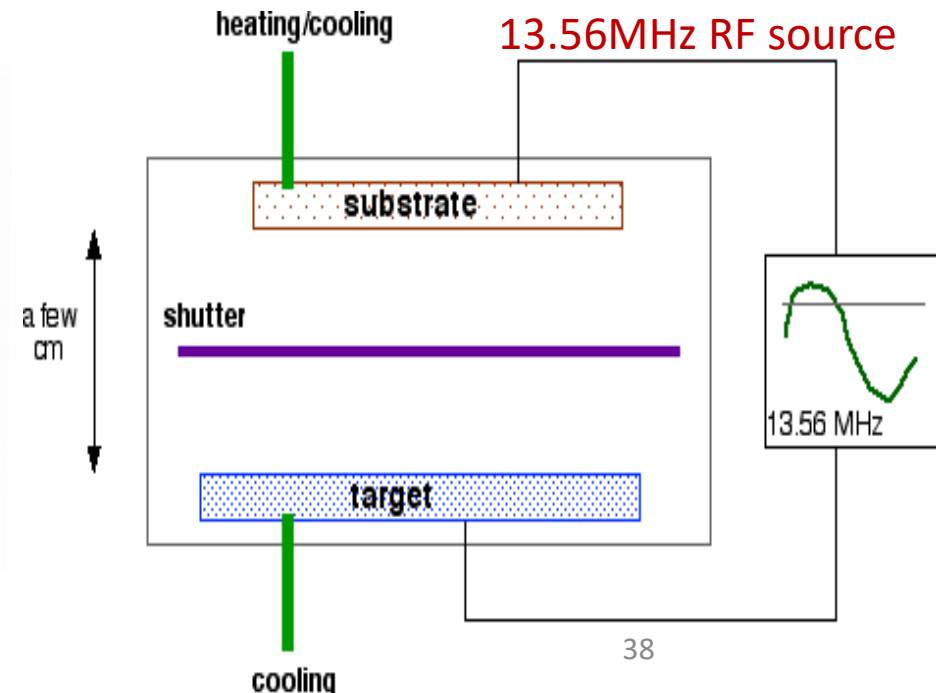
Figure 12.21 Cross section of the time evolution of the typical step coverage for unheated sputter deposition in a high aspect ratio contact.

RF (radio frequency) sputter deposition

- **Good for insulating materials because, positive charge (Ar^+) build up on the cathode (target) in DC sputtering systems. Alternating potential can avoid charge buildup**
- When frequencies less than $\sim 50\text{kHz}$, both electrons and ions can follow the switching of the anode and cathode, basically DC sputtering of both surfaces.
- **When frequencies well above $\sim 50\text{kHz}$, ions (heavy) can no longer follow the switching, and electrons can neutralize positive charge buildup on each electrode during each half cycle.**
- As now electrons gain energy directly from RF powder (no need of secondary electrons to maintain plasma), **and oscillating electrons are more efficient to ionize the gas, RF sputter is capable of running in lower pressure (1-15 mTorr), so fewer gas collisions and more line of sight deposition.**



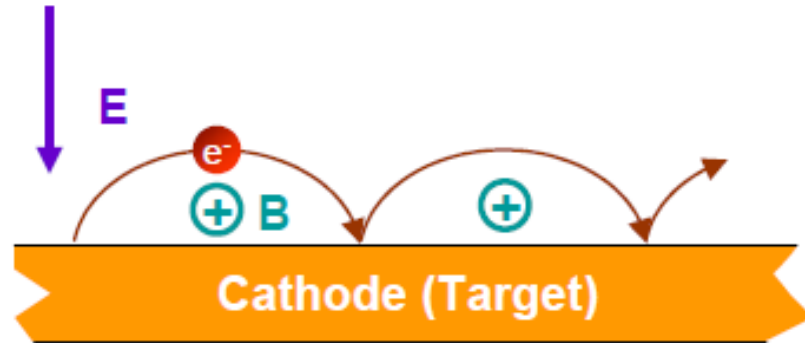
Switch polarities before the target surface saturates with ions.



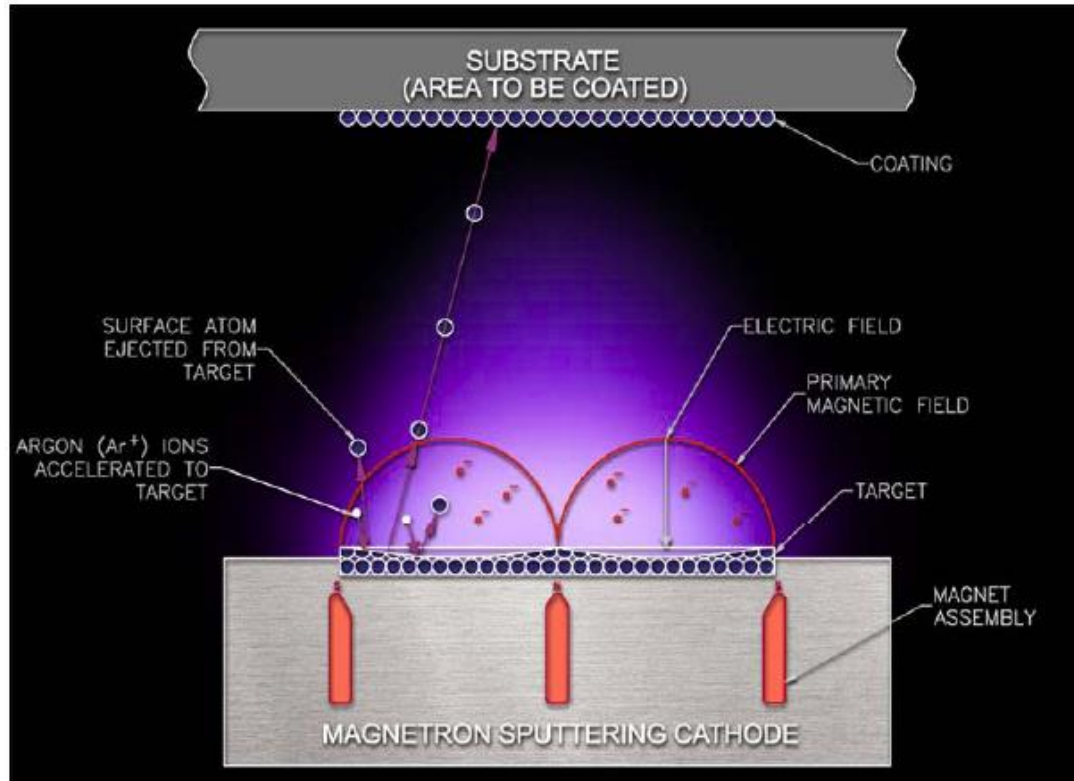
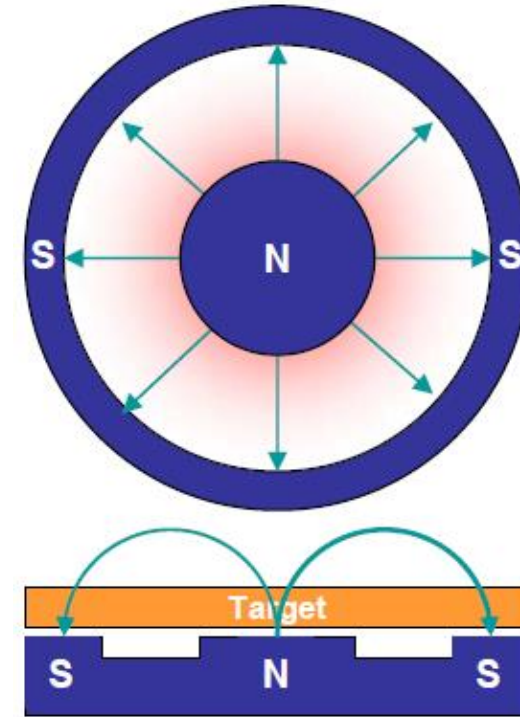
Magnetron sputtering

- **In DC & RF sputtering, the efficiency of ionization from energetic collisions between the electrons and gas atoms is low.**
- Most electrons lose energy in non-ionizing collisions or are collected by the electrodes.
- **Oscillating RF fields increasing ionization efficiency marginally.**
- **Hence, deposition rates are low.**
- **To increase deposition rates, magnets are used to increase the percentage of electrons that take part in ionization events, increasing the ionization efficiency.**
- A magnetic field is applied at right angles to the electric field by placing large magnets behind the target.
- **This traps electrons near the target surface and causes them to move in a spiral motion until they collide with an Ar atom.**
- **The ionization and sputtering efficiencies are increased significantly - deposition rates increase by 10-100×, to 1 μm per minute.**
- Unintentional wafer heating is reduced since the dense plasma is confined near the target and ion loss to the wafers is less.
- **A lower Ar pressure (to 0.5mTorr, can still sustain plasma) can be utilized since ionization efficiency is larger which can improve film quality as less argon will be incorporated into the film.**
- Magnetron sputtering can be done in DC or RF, but more often it is done in DC as cooling of insulating targets is difficult in RF systems.

Magnetron sputtering



Orbital motion of electrons increases probability that they will collide with neutral species and create ions.



Magnetron sputtering for high density of plasma near target.

Impact of magnetic field on ions

Hopping radius r :

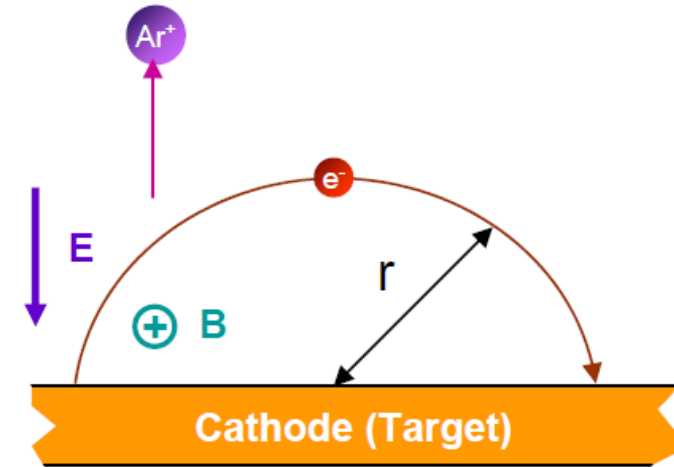
$$r \sim \frac{1}{B} \sqrt{\frac{2m}{e} V_d}$$

V_d : voltage drop across dark space/sheath ($\sim 100\text{V}$)

B : magnetic field ($\sim 100\text{G}$)

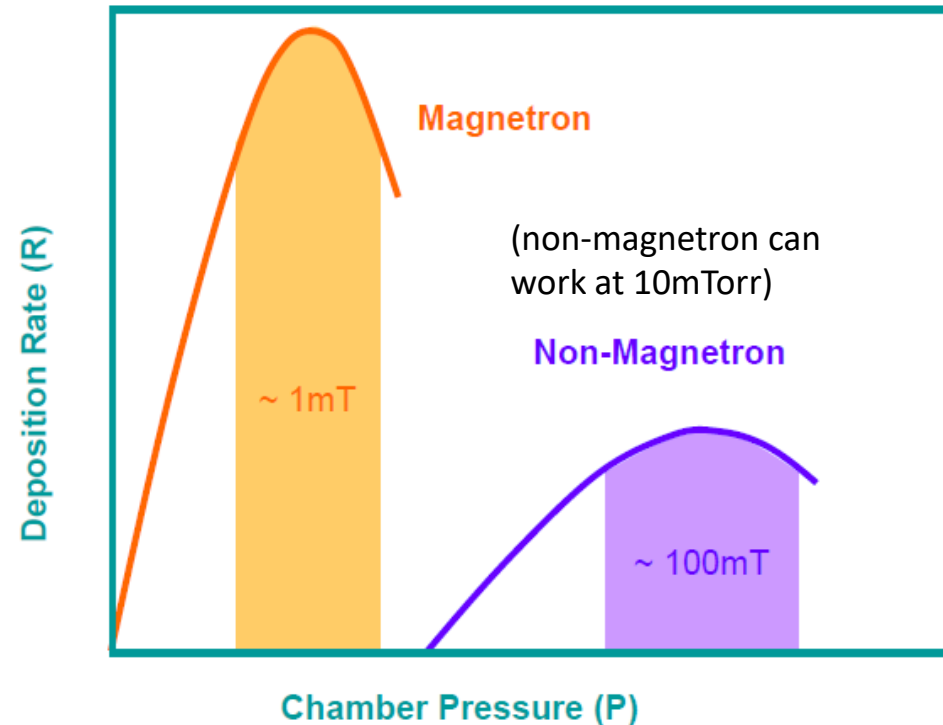
For electron: $r \sim 0.3\text{cm}$

For Ar^+ ion: $r \sim 81\text{cm}$



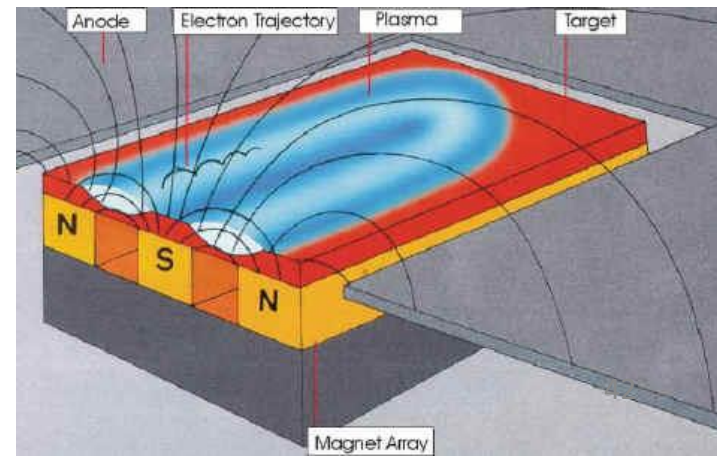
As a result:

- Current density (proportional to ionization rate) increases by 100 times.
- Required discharge pressure drops 100 times.
- Deposition rate increases 100 times.



Issues for magnetron sputtering:

Erosion track in the target, leading to poor target use efficiency and non-uniform film on substrate.



Comparison of evaporation and sputtering

Property	Evaporation	Sputtering
Rate	1000 atom layers/s	ca 1 atom layer/s
Thickness control	possible	easy
Materials	limited	almost unlimited
Cleanness	good	good
Substrate heating	no	yes
Surface roughness	little	ion bombardment
Selfcleaning	not possible	pole reversal
Multilayers	different holders	different targets
Adhesion	medium	good
Shadowing effects	large	small
Film properties	difficult to control	can be controlled
Equipment cost	medium	expensive

Comparison of evaporation and sputtering

EVAPORATION	SPUTTERING
low energy atoms	higher energy atoms
high vacuum path <ul data-bbox="366 679 1021 872" style="list-style-type: none">• few collisions• line of sight deposition• little gas in film	low vacuum, plasma path <ul data-bbox="1192 679 1964 872" style="list-style-type: none">• many collisions• less line of sight deposition• gas in film
larger grain size	smaller grain size
fewer grain orientations	many grain orientations
poorer adhesion	better adhesion

Comparison of evaporation and sputtering

Evaporation	Sputtering
Low energy atoms (~ 0.1 eV)	High energy atoms / ions (1 – 10 eV) <ul style="list-style-type: none">• denser film• smaller grain size• better adhesion
High Vacuum <ul style="list-style-type: none">• directional, good for lift-off• lower impurity	Low Vacuum <ul style="list-style-type: none">• poor directionality, better step coverage• gas atom implanted in the film
Point Source <ul style="list-style-type: none">• poor uniformity	Parallel Plate Source <ul style="list-style-type: none">• better uniformity
Component Evaporate at Different Rate <ul style="list-style-type: none">• poor stoichiometry	All Component Sputtered with Similar Rate <ul style="list-style-type: none">• maintain stoichiometry

Comparison of typical thin film deposition technology

Process	Material	Uniformity	Impurity	Grain Size	Film Density	Deposition Rate	Substrate Temperature	Directional	Cost
Thermal Evaporation	Metal or low melting-point materials	Poor	High	10 ~ 100 nm	Poor	1 ~ 20 A/s	50 ~ 100 °C	Yes	Very low
E-beam Evaporation	Both metal and dielectrics	Poor	Low	10 ~ 100 nm	Poor	10 ~ 100 A/s	50 ~ 100 °C	Yes	High
Sputtering	Both metal and dielectrics	Very good	Low	~ 10 nm	Good	Metal: ~ 100 A/s Dielectric: ~ 1-10 A/s	~ 200 °C	Some degree	High
PECVD	Mainly Dielectrics	Good	Very low	10 ~ 100 nm	Good	10 - 100 A/s	200 ~ 300 °C	Some degree	Very High
LPCVD	Mainly Dielectrics	Very Good	Very low	1 ~ 10 nm	Excellent	10 - 100 A/s	600 ~ 1200 °C	Isotropic	Very High